Interreg
North Sea Region
Building with Nature

Ministry of Environment and Food of Denmark
Coastal Authority

Aeolian Sediment Transport and Natural Dune Development, Skodbjerge, Denmark

January 2020

Project	Building with Nature (EU-InterReg)
Start date	01.11.2016
End date	01.07.2020
Project manager (PM)	Ane Høiberg Nielsen
Project leader (PL)	Per Sørensen
Project staff (PS)	Henrik Vinge Karlsson and Britt Gadsbølle Larsen
Time registering	402412
Approved date	27.01.2020
Signature	

Report	Aeolian sediment transport and natural dune development, Skodbjerge, Denmark.
Author	Henrik Vinge Karlsson and Britt Gadsbølle Larsen
Keyword	Aeolian sediment transport, Aeolian sedimentary budget, Skodbjerge, Dune development, Building with nature,
Distribution	www.kyst.dk, www.northsearegion.eu/building-with-nature/
	Kystdirektoratet, BWN Krogen, 2018
Referred to as	Kystdirektoratet (2020), Aeolian sediment transport and natural dune development, Skodbjerge, Denmark. Lemvig.

Abstract

This study is part of the EU-InterReg project Building with Nature. The focus of this report is the natural development of a 3.7 km dune stretch at Skodbjerge located on the North Sea coast of Denmark. Since 2005, the designated study area has been subject to high-resolution digital elevation mappings (DEMs). The DEMs derive from LIDAR scans and serve as primary data resource throughout this report.

Previous analyses of the coast assume that sediment accumulation inland of the dune top could be disregarded when analyzing the sedimentary budget of the coast, as the volumes in question were considered insignificant. The analysis of this report suggests otherwise, as considerable amounts of sediment accumulated in the area leeward of the dune crest during the study period. Findings are based on the changes in elevation over time, obtained by analyzing the DEMs and thereby determining the sedimentary budget between dune face and dune leeside. Furthermore, analyses on how natural dune development affects the safety level in the study area (40 m dune width at the 4.5 m contour) are included. The impact from the sea was originally meant to be excluded, as this report focuses on aeolian sediment transport and dune development, and the goal was to restrict the boundaries of the study area to the zone where only aeolian sediment transport occurs. This could not be fully achieved as acute marine erosion caused by storm surges were found to erode the dune face on multiple occasions along the study area. As these changes are natural influences and impossible to filter out when using planimetric boundaries, they are accepted in the study.

The results of the analyses showed that a considerable amount of sediment accumulates inland of the dune crest, and that the sedimentary budget between erosion of the dune face and accumulation at the dune lee side is almost balanced. Generally, there is a slight volume surplus during the study period, despite an overall narrowing of the dune width at the 4.5 m contour.

Analyses of spatial variations showed that accumulation primarily takes place in depositional lobes of blowouts and leeward of the dune crest. Volume generally increases along the total stretch of dunes analyzed. Erosion primarily takes place at the dune face and in the deflation basins of blowouts. It was found that some parts of the dune stretch were exposed to large erosion of the dune face, which was caused by local marine erosion. The dune face 4.5 m contour retreated in most of the study area but the leeside 4.5 m contour did, in some areas, migrate inland, thus minimizing the decrease in dune width and safety level.

Analysis of temporal changes in the study area showed that there are significant differences during the study period as regards mass movement. Periods with low accumulation rates and low erosion rates, periods with significant accumulation and low erosion, as well as periods with low accumulation and high erosion were encountered between 2006 and 2019. Therefore, no consistency in erosion/accumulation over time can be detected, and it becomes clear that several factors affect dune development and aeolian transport.

As there are differences in time between the LIDAR scans, a normalization of volume change over time was of interest. A linear correlation test was performed between volumes of erosion/accumulation and the number of hours with wind speeds above a critical threshold fluid velocity for initiation of grain movement. The test showed low correlation between the two, which confirms that aeolian sediment transport is a complex process in which many factors, other than the wind velocity, affect the actual aeolian transport rate and dune development.

Contents

1. Introduction

1.1 Background

This report is a part of the EU-InterReg project Building with Nature. The overall objective of Building with Nature is to improve coastal adaptability and resilience to climate changes by means of natural measures. Being a partner in the project, the Danish Coastal Authority (DCA) analyse different aspects of using natural processes and materials in coastal laboratories on Danish coasts. This project seeks to improve our understanding of the processes and interactions within the coastal system.

The research for this part of the Building with Nature project primarily relates to the dune area. Research in other parts of the project relates to the rest of the active profile ranging from the active depth, where the waves start to affect the seabed, to the beach and the dune area, which is affected by storm surges and wind. Thus, the Building with Nature project covers the entire active part of the coastal profile. The source-pathway-receptor model (SPR) supports this approach, which focuses on the entire active coastal system, including the interdependent parameters. The sources are for example wind, waves, tide, marine surge and current. The pathway is the coastal profile from the shore face across the beach to the dunes. Infrastructure, vacation homes, protected nature etc. are the receptors. By modification of the pathway such as for example shore face nourishments, beach nourishment, dune reinforcement, planting of vegetation, building of fascines etc., it is possible to maintain or increase the coastal resilience and the safety level to protect the receptors against flooding and erosion.

1.2 Objectives

The objective of this study is to build more evidence on the natural morphological changes and sedimentary budget of dunes in order to assess coastal resilience and natural variations in the safety level. Insights into these processes and the resulting morphological dune changes are useful for modification of pathways in order to provide safety utilizing nature's own forces, processes and materials to stabilize and build-up dunes. Moreover, concerning dunes, building with nature methods are of special interest because they allow the dune ecosystem to be preserved. This is not the case when using traditional passive coastal protection methods.

Since the dune is a natural barrier against flooding of the low-lying hinterland and acts as a buffer of sediment in case of erosional events, it is relevant to investigate the dune evolution in order to gain a more complete understanding of the system. Dunes are natural elements of coastal areas and their development are based on natural processes, which means the dune system is dynamic and safety level provided by the dunes varies over time. Blowouts are common morphological features in the dune area. Deflation basins of blowouts can cause large changes in the foredune due to aeolian processes that transport sediment further inland where it is often deposited in depositional lobes. It is therefore an aim of this study to assess the natural effect of blowouts in dune areas. The understanding of the morphological and volumetric changes of the dune system can be utilised when designing building with nature methods for future coastal protection.

Furthermore, it is an objective of this study to analyse the amount of sediment transported across the dune top and into the area leeward of the dune crest, as this sediment sink is often neglected when calculating the sedimentary budget of a coastal area.

1.2.1 Hypotheses

The objectives of the study have led to the following hypotheses:

- Accumulation of sand in the dune area is primarily found on the lee side of the dune crest and in the depositional lobe of blowouts. Erosion is primarily found at the dune face and in the deflation basin of blowouts.

- The wind climate affects the amount of sediment eroded and accumulated in the dune area. The shape and orientation of the accumulated sediment reflect the dominating wind direction
- Aeolian transport of sediment and the presence of blowouts can cause considerable changes in the dune area, which in turn affects the safety level.

1.2.2 Research questions

In order to further investigate and test the above-mentioned hypotheses the following research questions were defined:

- Which areas of the dune are dominated by erosion and accumulation, respectively?
- What are the effects of the wind climate on development of the dunes?
- Do volume and dune morphology change during the study period and is development on the lee side equivalent to that of the dune face?
- How does aeolian sediment transport and dune development affect the safety level?
- How does the sedimentary budget of the dune area contribute to the overall profile development and the general coastal sedimentary budget?

1.3 Safety Level prescribed in the Joint Agreement from Lodbjerg to Nymindegab

The Danish Government and the local municipalities have signed a joint agreement to protect coastal areas between Lodbjerg and Nymindegab on the Danish North Sea coast. Skodbjerge is located within this area. The Joint Agreements are financial agreements usually covering a five year period and the agreement will be up for renegotiation every 5 years.

The overall purpose of the Joint Agreement is to ensure that the dunes on these coastal stretches are resilient enough to withstand erosion and winter storms and prevent a breach during a storm with a 100 year return period. The only exception is Thyborøn where the objective is protection against a 1000 year storm event.

The coastal stretch included in the Joint Agreement is divided into subareas. Dune safety criteria are defined for these subareas, and they specify minimum dune heights and minimum dune widths based on the surveys and analyses made by the Danish Coastal Authority. Furthermore, it is a goal either to reduce or stop the coastal retreat of the active coastal profile from the dune top to -6 m (Figure 1-1).

In order to be able to withstand a storm with 100 or 1000 (Thyborøn) year return period, the coast must have an assigned minimum dune width and a minimum dune height. The minimum dune heights are based on the water level of a storm with 100 year return period (1000 year return period in Thyborøn). At Skodbjerge the minimum dune height is 4.5 m.

The minimum dune width is 40 m measured at the minimum dune height. However, if a revetment is present in the dune, the minimum dune width is 30 m. At Skodbjerge, the minimum dune width is 40 m, measured at the height of 4.5 m.

Whether it is a goal to reduce or stop the coastal retreat depends on the safety buffer present at that particular coastal stretch and the neighbouring stretches. At Skodbjerge there is an extra buffer in the dune and therefore the goal is to reduce the coastal retreat to 1 m per year (Figure 1-1). On stretches

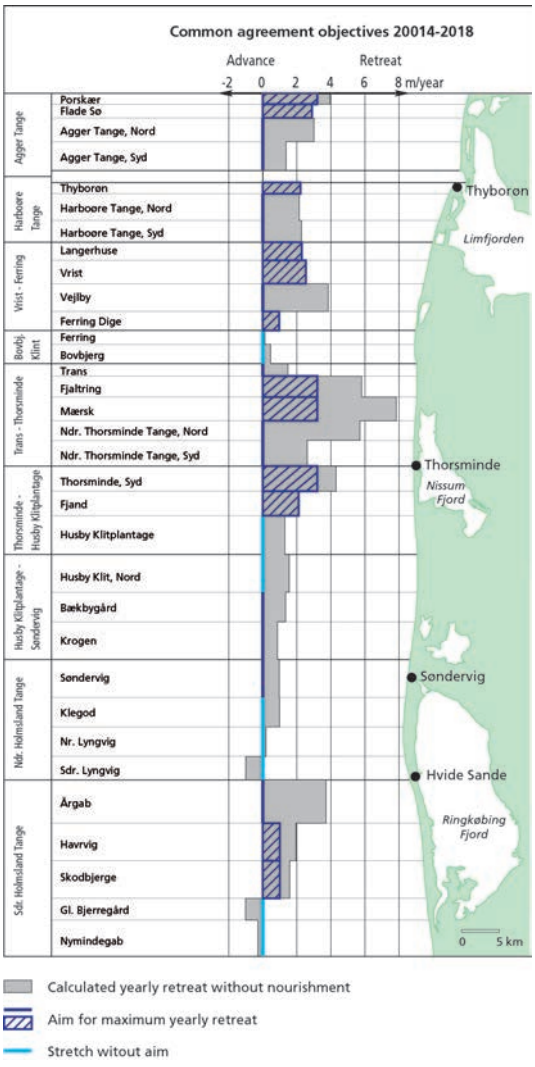

Figure 1-1. Goals for the area of the Joint Agreement from Lodbjerg to Nymindegab. The grey area indicates the calculated annual coastal retreat without nourishment. Dark blue indicates the goal for maximum annual coastal retreat. Light blue indicate areas without a goal.

with a revetment, the goal is to reduce the coastal retreat as much as possible within the economic framework of the Joint Agreement.

1.4 Dune terminology

The dune area and morphology consist of several different elements. The terminology used in this report is presented in Figure 1-2.

Dune crest is easily detected if the dune is scarped, the dune crest will then be the point from which the vegetation becomes consistent. In Figure 1-2, the dune crest is easily detectable. Another way to determine the crest in a transgressive dune is to determine the point that over years separates the seaward area of erosion and a landward area of accumulation.

Dune top is the highest point in the foredune. This might coincide with the dune crest (as in Figure 1-2) but this is not always the case.

Dune toe is often referred to as the point where abrupt slope change takes place between the beach and the dune due to scarping from maximum water level. The dune toe is often very visible after a storm. However, in the period that follows, accumulation due to aeolian sediment transport will create a ramp between beach and dune which will cover the dune toe. In other reports, the dune foot is defined as the maximum 1 year statistical high water level (Ries, 2019), or a distinct contour corresponding to the maximum wave run up.

Dune heel can be defined as the point between the dune lee side and the flat hinterland where the slope decreases significantly.

Dune face is the part of the dune between dune crest and dune toe. Generally, it defines the area of the dune that is facing the sea.

Dune lee side is the area from dune crest to the dune heel. The dune top will therefore be part of the lee side.

Stoss side defines the surface where wind creates traction and friction, which can mobilize sand grains. The position is therefore very dynamic and variable over time, but generally describes dune areas facing the sea as the predominant wind direction is west.

Foredune is the dune ridge consisting of a dune face, dune crest/top and a dune lee side. Seen from above the seaward boundary is the dune toe and the landward boundary is the dune heel.

The swale is a longshore parallel through separating foredunes and inactive inland dune ridges. This area is vegetated. The swale is not present along the entire stretch of the study area.

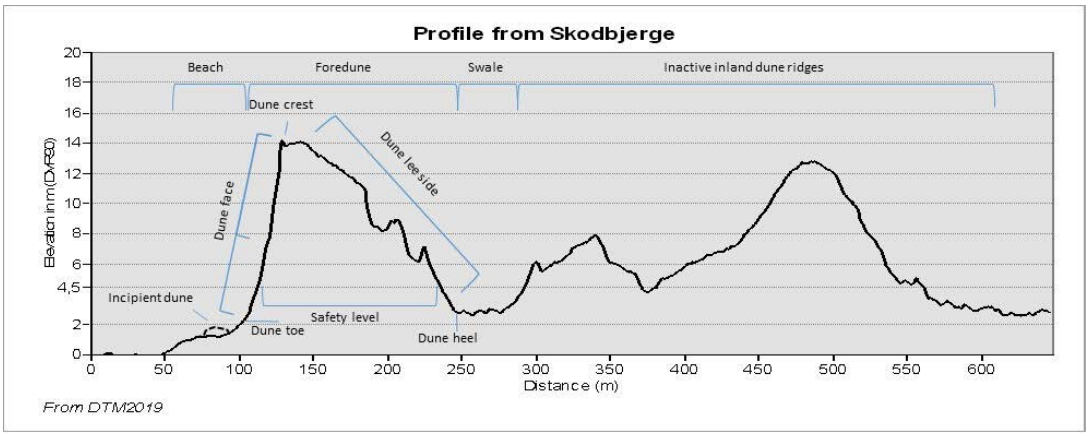

Figure 1-2: Morphological zones of the profile illustrating the terminology used for this report. The transect is derived from the DTM2019 and is representative for Skodbjerge.

2. Study area

The Danish North Sea coast at Skodbjerge is a micro tidal wave dominated, sandy coast. The coast is highly dynamic and the morphological changes adjust to climatic conditions. Large alongshore variations in the coastline have been documented along the study area, rhythmic bar systems and separating rip currents create coastline perturbations and indentations, which migrate as the bar system migrates alongshore in the sediment transport direction, which is southbound (DCA Systems Description, 2018).

Figure 2-3 shows the study area of Skodbjerge, which has a total length of 3.7 kilometres. Skodbjerge is located on the southern part of the narrow spit, Holmsland Tange, which encloses Ringkøbing Fjord. The main road Sønder Klitvej is the only road connecting the southern part of the spit with the northern Holmsland Tange. Along Sønder Klitvej there are several areas with vacation homes in the dunes. The road runs parallel to the coast about 800 m inland.

The 20 year and 100 year storm return water levels are 2.57 meter and 2.74 meter. The chronic erosion at Skodbjerge is about 2 m/yr. Acute erosion can result in a retreat of the dune face of more than 10 m during a single storm event. There is no hard coastal protection in the study area. The naturally developing dunes are in sections 1, 2, and 3 backed by a plateau formed by a dune reinforcement established in 1994. Beach nourishments and beach scraping have been carried out several times during the 1990's, but the only coastal protection performed during the study period consists of shoreface nourishments in 2010 and 2011.

Figure 2-2: Drone image from March 28 2019. A large deposit of aeolian transported sediment is visible in the area leeward of the dune crest.

Figure 2-1: Drone image from July 23 2019. Substantial variation in vegetation cover in the area landward of the dune crest when compared to the drone image taken 4 months earlier.

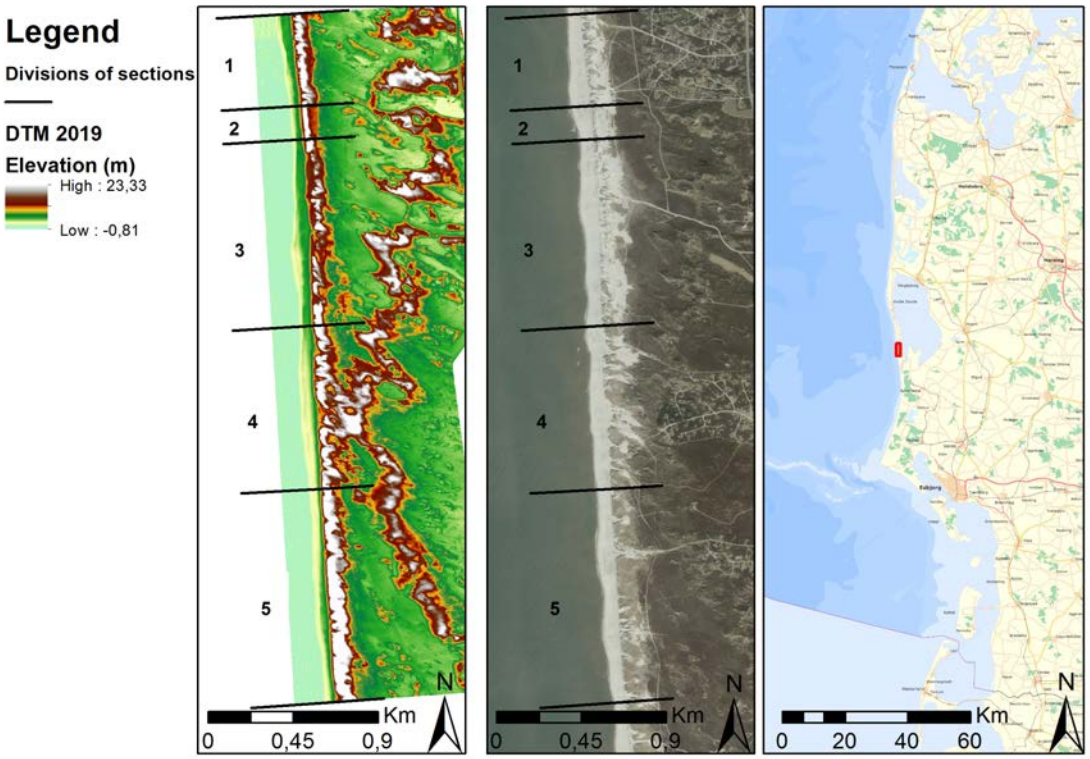

Figure 2-3: Study area of Skodbjerge located at the Danish North Sea coast. The study area is divided into 5 alongshore sections based on different morphological characteristics.

The dunes at Skodbjerge are generally steep, with variations within the study area. Dunes in the northern part of the area have the steepest dune faces while the widest dune sections are in the southern part of the coastal stretch. The study area is highly affected by aeolian sediment transport and wind-scoured blowouts which creates a dynamic dune area. An example of this is shown in the drone images taken on March 28 2019 and July 23 2019 (Figure 2-2 and Figure 2-1) showing that the area has changed significantly through these 4 months. The vegetation in the dunes consists primarily of marram grass. In the hinterland of the foredune there is a greater variety of vegetation types, this will not be covered by this report as it is outside the study scope.

2.1 Sections

For a more detailed description and analysis of the morphological changes within the study area it has been divided into five subareas (section 1-5) of varying length. The division is based on morphology and dune development (Figure 2-3). The study area of Skodbjerge has a total length of 3.7 kilometres.

Section 1 is 490 m long and the dunes are approximately 12-13 m high (2006). A dune reinforcement in 1994 resulted in a plateau at 6 m DVR90 in the dune leeside. This plateau can be identified from orthophotos taken between 1995 and 2006, as well as from LiDAR scans and cross sections of the dune. Above 6 m DVR90 the foredune is relatively narrow. In section 1, many relatively small blowouts are present in the foredune. Furthermore, this section is the only section where accumulation dominates the beach and the profile below 4 m DVR90 during the study period.

Section 2 is 180 m long and the dunes are approximately 14-15 m high (2006). This section is also affected by the dune reinforcement performed in the area in 1994, which means that the dune is relatively narrow above the 6 m contour, whereas the dune is wider below the 6 m contour creating a plateau. Section 2 is characterized by having a very regular foredune almost without blowouts. Only one small blowout is present.

Section 3 is 990 m long and the dunes are approximately 14-16 m high (2006). This section is also affected by the dune reinforcements carried out in 1994, as they created a plateau at the dune leeside. The native dune has migrated inland over the reinforcement. This is caused by the presence of blowouts. This results in an irregular dune face. Despite the significant retreat of the top of the dunes along 540 m of the stretch, a ridge of sediment is present in connection with the adjacent dunes in the original position of the dune top. This ridge appears man made, but there are no indications from historical sources (neither in reports nor in orthophotos) that it should be so, and it is therefore assumed to be a natural morphological feature. At this point there is little knowledge on the development of this morphological feature but it is suggested that the stone paved ridge is the result of accumulations of pebbles and stones during storm events.

Section 4 is 870 m long and the dunes are approximately 13-15 m high (2006). This section is dominated by large blowouts. Some of the blowouts are very close to each other, creating a coalesced area of blowouts. Landward of the foredune ridge an older dune ridge meets the foredune at an oblique angle from behind. These dunes are inactive grey dunes (Figure 2-3) but due to their presence and height, section 4 is the widest section at the 4.5 m contour.

Section 5 is 1140 m long and the dunes are 14-18 m high (2006) with the highest dunes located furthest to the south. In section 5 large blowouts are present, but they are more separated than the blowouts in section 3 and 4. Despite section 4 being the widest at the 4.5 m contour, section 5 represent the highest and most regular dune ridge.

For a more detailed description of the study area of Skodbjerge, see Systems Description of Skodbjerge (Kystdirektoratet, 2018).

3. Theory

The dune area is a highly dynamic landscape, which is continuously developing, and it is no simple task to grasp the variety and complexity of it. However, the following chapter seeks to provide a brief introduction to the main elements of aeolian sediment transport and the processes affecting dune formation and dune development.

3.1 Dune formation

Wind creating aeolian transport of sediment is the main source of sediment supply for building of foredunes on sandy beaches. For dunes to form there needs to be a sufficient supply of finer sediment and wind energy above a minimum threshold velocity for aeolian sediment transport. Moreover, the dune development is affected by the presence of pioneer plants on the backshore (Hesp, 2011). When the wind creates a landward transport of sediment from the beach the sediment is trapped in the vegetation that is colonizing the area landward of the limit for wave action during storm. This leads to development of a foredune ridge parallel to the shoreline (Davidson-Arnott, 2010). On beaches where the sediment supply is limited or where there is a low frequency of strong onshore winds, a single foredune can develop. In areas with abundant supply of sediment and strong onshore winds a more complex dune field can develop either by means of inland migration of dunes or by progradation of the shoreline and formation of successive foredune ridges (Davidson-Arnott, 2010).

3.2 Flow dynamics

Local topography of the dune area can modulate the regional wind fields, causing a complex flow near the surface, and thereby affect the resulting sediment transport.

When the wind encounters the stoss slope of the dune, the wind flow is topographically accelerated due to compression of the flow, which cause accelerated wind speed on stoss slopes and over dune crests (Hesp, 2011). This is known as topographic forcing. The wind speed is lowest at the dune toe and increases up the stoss slope (Bauer, et al., 2012). As the flow accelerates towards the dune crest, the sediment transport typically increases (Walker, et al., 2006). A zone of stagnation with lower wind velocities may be generated near the dune toe, and this can lead to accumulation of sediment at the dune toe. Topographic forcing is strongest when the wind direction is perpendicular to the foredune and decreases as the wind direction becomes more oblique.

At the dune crest the wind direction and the topography determine whether the flow remains attached or a zone of flow separation is developed (Davidson-Arnott, 2010). Flow separation is common over dune crests and lee slopes of dunes. The separation envelope at the leeslope of the dune, reversing flow, and reduced wind velocity causes sediment deposition leeward of the dune crest (Hesp, 2011). Figure 3-1 shows a foredune where the wind direction is onshore and the flow is detached and a zone of flow separation is developed (Bauer, et al., 2012).

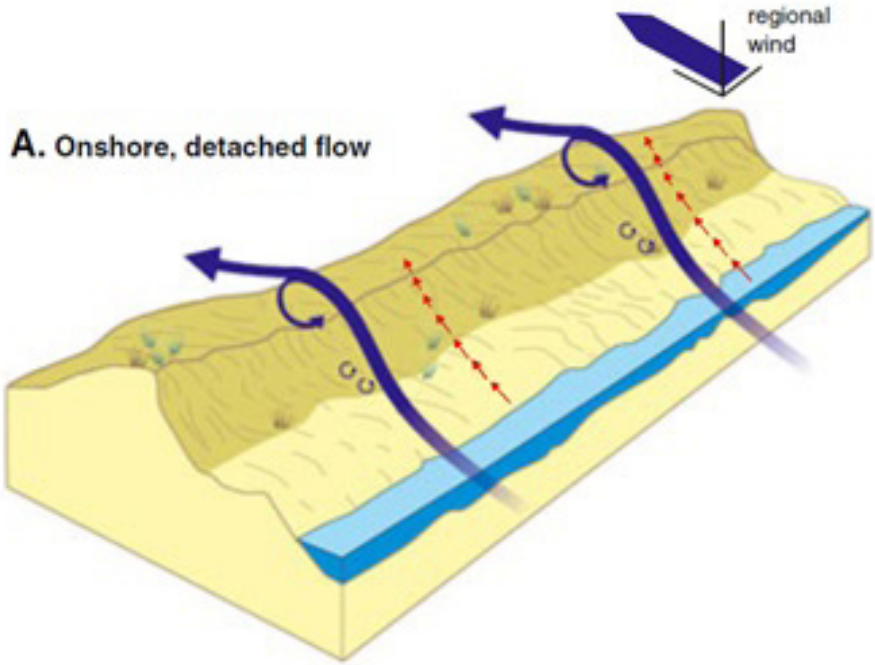

Figure 3-1 Conceptual model of flow over a large foredune (> 8 m). The wind direction is onshore, the flow is detached and a lee-side recirculating eddy develops. The blue arrow illustrates the near-surface wind flows steered by the local topography. Red arrows illustrate the likely sediment transport direction (Bauer, et al., 2012).

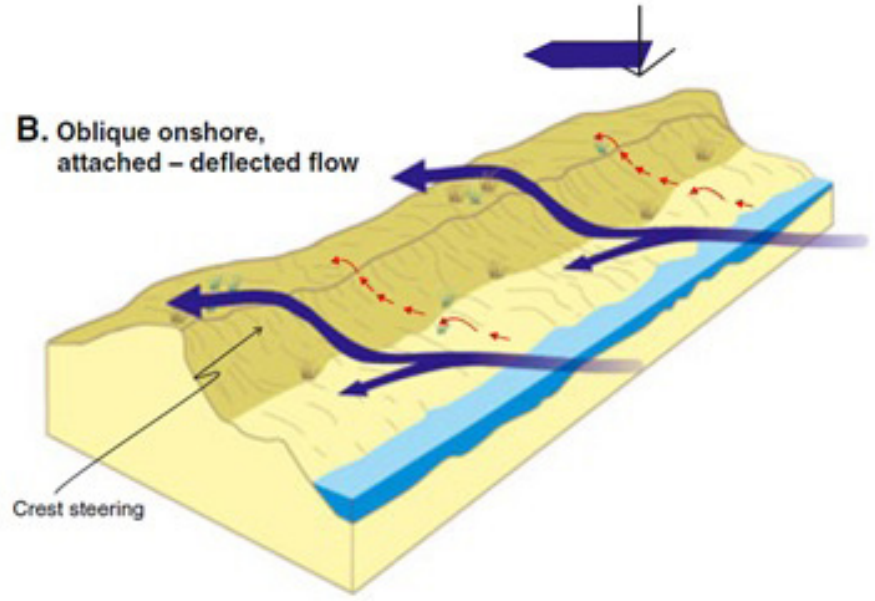

Figure 3-2: Conceptual model of flow over a large foredune (> 8 m). The wind direction is obliquely onshore, the flow is attached and the flow is reflected due to topographic steering. The blue arrow illustrates the near-surface wind flows steered by the local topography. Red arrows illustrate the likely sediment transport direction (Bauer, et al., 2012).

Topographic steering of near surface winds can cause deviations in the flow that can be significantly different in direction and magnitude from the regional wind. Wind approaching the dune at an oblique angle (30° to 60° to the dune crest) will often be deflected toward crest-normal while winds from directions less than 30° to the dune crest will be deflected parallel to the foredune (Walker, et al., 2006). Figure 3-2 shows a foredune where the wind direction is obliquely onshore and the flow is attached and deflected (Bauer, et al., 2012).

3.3 Marine erosion

The dune area is mainly affected by aeolian processes but during storm surges high water levels, waves and currents can cause severe acute erosion of the dune toe and the dune face. However, storm events are separated by much longer periods where only aeolian processes cause dune development.

After a storm event, when marine processes have caused erosion of the dune face and transported sediment seaward, the post storm profile is often a relatively low, flat profile with a steep dune face and a

distinct dune toe due to dune scarping. When marine processes cause acute erosion of the dune toe the dune stoss slope steepens and the dune can be exposed to slumping where sediment destabilizes and accumulates at the dune toe. From here, it becomes available for further transport by waves. When the wave conditions and water level normalize after a storm, sediment is transported towards the beach and from the beach aeolian processes can transport sediment towards the dune area. To some extent, this allows the dune to recover from the acute erosion if time allows before next storm event.

As aeolian sediment is transported towards the dune toe, a dune ramp can be formed and the stoss slope becomes less steep. Presence of a dune ramp is of great importance to the sediment transport from the beach to the dune and leeward of the dune crest. Aeolian sediment transport over the dune crest increases as the height of the dune ramp relative to the dune crest increases (Christiansen & Davidson-Arnott, 2004).

3.4 Blowouts

A blowout is a depression formed by the wind on a pre-existing sand deposit (Hesp, 2011). The morphology of blowouts is highly dynamic. Blowouts typically consist of a deflation basin in which wind processes erode sediment and transport it further downwind, creating a depositional lobe by accumulation of sediment. In many dune areas blowouts are the main feature of aeolian sediment transport (Jungerius, et al., 1991).

Blowouts are common in coastal dune areas, especially in areas where the beach is receding and in high energy environments (Hesp, 2011). Blowout formations initiate in different ways e.g. by wind erosion of patches with sparse vegetation, local flow acceleration caused by the topography, marine erosion of the dune face and dune toe followed by aeolian transport of sediment from areas without vegetation, and human activities in the dune (Hesp, 2011; Davidson-Arnott, et al., 2008). Studies have shown that the largest development of blowouts do not take place during the largest onshore storm events but are more likely to be caused by lower wind velocities with a higher frequency (Jungerius, et al., 1991).

3.5 Initiation of aeolian sediment transport

The following section presents equations for calculations of the wind speed needed for initiation of grain movement in not cohesive sediments. In order for sand grains on the beach to move along and across the beach into the dunes, the threshold shear velocity must be attained. For the sand grains on the surface to initiate movement, the vertical drag on the single sand grain must exceed the forces keeping it on the surface.

The threshold shear stress (v_{*t}) for movement of a dry grain is presented by Bagnold as:

$$v_{*t} = A\sqrt{\frac{\sigma - \rho}{\rho} * gd}$$

Where A is an empirical factor (in air set to 0.1 and close to constant for grain sizes above 0.025 cm (Bagnold, 1954)), σ is density of the sand grains (2650 kg/m³ for quartz), ρ is density of the air (1.25 kg/m³), g is the gravitational acceleration (9.81 m/s²), d is grain diameter.

As this equation merely expresses the required speed of the wind at the surface in order to initiate movement, it must be converted into a defined height above ground.

In the following equation the fluid velocity (v) in a given height (z) is related to the surface roughness constant ("k" defined as d/30), drag force (τ) per unit area and the drag coefficient for the grain $\left(V_* = \sqrt{\frac{\tau}{\rho}}\right)$

$$v_z = 5.75 * V_* * \log\left(\frac{z}{k}\right)$$

The value 5.75 is the factor of proportionality between wind velocity and the logarithmical height of the wind measure determined in (Bagnold, 1954).

The threshold fluid velocity (v_t) at a given height (z) can then be estimated by substituting the drag coefficient (V_*) with the expression for the threshold shear stress (v_{*t}) in the above, which results in the following relation:

$$v_t = 5.75 * A \sqrt{\frac{\sigma - \rho}{\rho} * gd} * \log\left(\frac{z}{k}\right)$$

Thereby the threshold wind velocity for initiation of grain movement at a given height above the surface (z) can be determined – From here on referred to as the critical threshold fluid velocity. A slightly different approach relies on "the law of the wall" (Masselink, et al., 2011) where the average wind speed at height (z) can be determined as:

$$U_z = \frac{u_*}{\kappa} \ln\left(\frac{z}{z_0}\right)$$

Where U_Z is the averaged wind speed at height (z), and κ being the Von Karmans constant estimated to 0.4 by Masselink, z_0 being the surface roughness (described as d/30 by Bagnold and named k) and u_* is the shear velocity (named drag coefficient by Bagnold). By substituting u_* with v_{*t}, the critical threshold fluid velocity (denoted U_t in (Masselink,et al.,2011)) at a given height above the surface (z) can be determined.

3.6 Aeolian sediment transport

When the critical threshold fluid velocity is reached and aeolian sediment transport is initiated, the grains are transported close to the bed by creeping. If the fluid drag increases, movement by saltation occurs, and the grains are moved forward by a series of jumps. These jumps initiate movement of other grains on the bed through impact. Suspension is the process of grains being carried by the wind over longer distances (Davidson-Arnott, 2010). Saltation is the dominating process causing aeolian transport. Figure 3-3 illustrates the different transport modes: creeping, saltation and suspension.

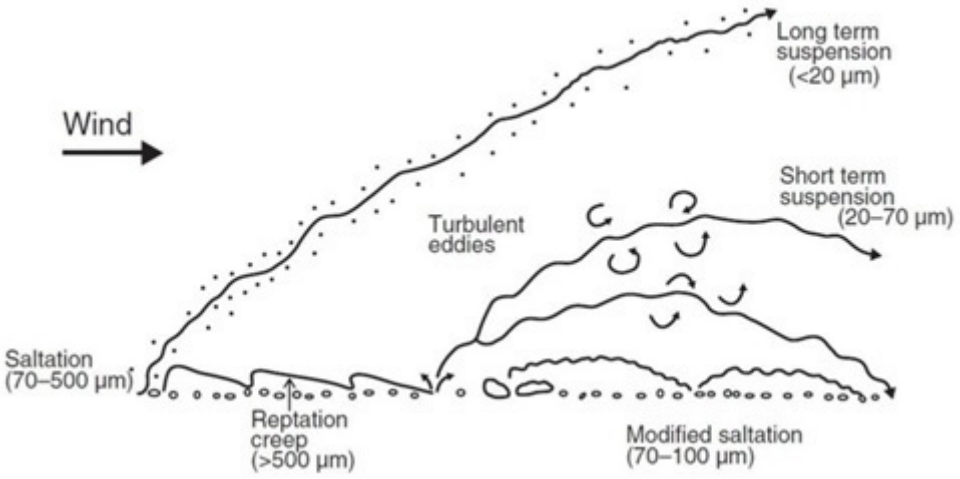

Figure 3-3 .Modes of aeolian sediment transport after Nickling and Davidson-Arnott, 1990 (Davidson-Arnott, 2010).

Deposition of the grains transported by the wind will occur when wind velocity decreases because of changes in the wind flow, interactions with the surface, presence of vegetation or other obstacles. On open surfaces without shelter, the grains will often be remobilized for further transport but if the grains are deposited in the lee of an obstacle, such as vegetation, the grains are sheltered and accumulation can occur. This deposition is limited by the height of the obstacle creating shelter. However, growth of the vegetation can often keep up with accumulation of sediment, which leads to growth of the dune (Davidson-Arnott, 2010). In this way, vegetation in dunes both serve to trap sediment and stabilize the dune, while allowing it to grow with the accumulation of sediment.

3.7 Constraining factors

Calculations of aeolian sediment transport often overestimate the transport rates because of different conditions, which constrain the entrainment of sand from the surface to the wind.

Aeolian sediment transport is typically constrained by effects such as moisture content (Davidson-Arnott, et al., 2008), lag deposits (de Vries, et al., 2014), vegetation and fetch length (Bauer, et al., 2009), which means that transport rates can vary in time independent of wind conditions.

Longer fetch lengths lead to higher transport rates until a certain limit is reached. This is the critical fetch where the wind is saturated. The distance the wind travels across the beach depends on the wind direction and the beach width. If the distance the wind travels across the beach is smaller than the critical fetch, variable beach widths lead to variable sediment transport rates towards the dunes (Bauer & Davidson-Arnott, 2002).

S. de Vries et al (2014) found that sediment transport on the beach is governed by spatial variations in sediment supply rather than wind speed. The aeolian sediment transport varied in time with the tide while the wind speed was constant. The study found that the intertidal zone can be a significant source of sediment for aeolian transport. Furthermore, this study found that presence of lag deposits can limit the sediment supply. When aeolian processes have transported fine grained sand away from the beach it can leave a layer of larger grains (lag deposits are displayed in Figure 3-4) which armour the surface of the beach and thereby decreases the amount of sediment available for aeolian transport (New Jersey Sea Grant Consortium, 2016). In order for these fine grains to become available for aeolian transport the sediment needs to be mixed by wave action.

Aeolian sediment transport is greatly affected by the surface moisture content of the beach, which can be described by processes in the intertidal zone, atmospheric humidity and precipitation (Bauer, et al., 2009). Moisture content limits the sediment supply, influence the threshold for sediment movement and decrease the transport rates (Davidson-Arnott, et al., 2008).

Another aspect in the dune development and natural change is simply the factor of time. The timescale on which we analyze is highly relevant in order to understand the dynamic behavior. The dunes along the North Sea coast of Denmark have been developing for centuries and millennial if counting the post-glacial developments. The time scale in which this study works is merely decadal and therefore the dynamic of these coast parallel dunes can vary over longer timescales than this study covers, e.g. in regards to climatic, geological as well as anthropogenic influences.

Figure 3-4: Lag deposits on a site known as Husby, Danish North Sea coast, March 28 2019.

4. Data

4.1 LiDAR

Once a year since 2005 a LiDAR (Light Detection And Ranging) scan have been conducted within the Joint Agreement stretch from Lodbjerg to Nymindegab on the central part of the North Sea coast of Denmark. The study area of Skodbjerge is situated in the southern part of the Joint Agreement stretch and LiDAR scans are therefore available for years between 2005 and 2019 with the exception of 2014.

LiDAR scans on the North Sea coast are done from airplanes. Laser beams are targeted at the surface, and the reflection of the beam back to the scanner is used for obtaining the distance between scanner and surface. Using global positioning system (GPS) and internal navigation system (INS) these distances can then be converted into a three-dimensional point in space, with x, y and z coordinates. The LiDAR scans consist of thousands of points, so they require post-processing to remove irrelevant material, such as birds, reflections etc. The result is a digital elevation model (DEM) which can be processed to represent a digital surface model (DSM) or if vegetation, buildings, bridges etc. are removed, it represents a digital terrain model (DTM).

Both DSM and DTM are available in raster formats from each of the scans but only DTM is included in analyses for this report.

	Date of measurement	DTM	Orthophoto	Point cloud
2005	May 24th	1.0 m	-	-
2006	March 30th	1.6 m	-	-
2007	March 29th	1.6 m	-	-
2008	May 15th	1.6 m	-	-
2009	March 29th	1.6 m	-	-
2010	September 3rd to 4th	1.6 m	-	-
2011	December 15th	0.5 m	-	-
2012	November 9th to 12th	1 m	20 cm	6-7 points pr. m²
2013	December 12th	1 m	20 cm	6-7 points pr. m²
2015	April 19th	1 m	5 cm	-
2016	April 11th	1 m	16 cm	8-9 points pr. m²
2017	April 19th	1 m	5 cm/10 cm	6-7 points pr. m²
2018	March 20th to April 11th	1 m	16 cm	-
2019	July 2nd to 16th	1 m	20 cm	-

Table 4-1: Information about each LiDAR scan. Date of measurements of LiDAR scan, cell size of DTM, resolution of orthophotos, number of points pr. m².

Table 4-1 shows the available information about cell size of the raster data sets, point cloud density, orthophoto resolution and sensing period. Vertical accuracy is within 5 cm and planimetric precision is within 15 cm. Not all information on the individual raster layers is available and the amount of points per m² is not known for all years. From 2012 to 2019 orthophotos have been taken during the scanning process.

4.1.1 Data validity

The DTM data sets are in raster format, which, despite comparable methods for post processing, come in different spatial resolutions (Table 4-1). As the resolution is often determined on point density requirements per m², the difference is likely to stem from differences between the requirements of the different contractors from year to year.

The sampling of terrain points for DTM creation are unknown and have been conducted by different contractors over time. Therefore, there may be variations in the methods used or the standard may have changed over time as LiDAR post-processing have evolved since 2005 and the quality of the data have improved.

The 2005 scan has been excluded based on erroneous data. Seemliness between mosaics in the scan is incomplete and generally contains "NoData" values. The scan from 2007 has also been excluded from this study, as it turns out to be tilting from North to South.

4.2 Wind

Wind measurements are available from Hvide Sande Harbour as 10 minutes averages measured approximately 25 m above surface and from Blaavand where wind measurements are available in 10 minutes averages from 10 m above terrain. Measurement stations in relation to the study area are shown in Figure 4-1. The measurements from Hvide Sande are conducted by the Danish Coastal Authority (DCA), while the Blaavand measurements derives from the Danish Metrological Institute (DMI). The Hvide Sande measurement station is only 10 to 13 kilometres away from the study area, while the Blaavand wind gauge is 40 kilometres away (Figure 4-1).

The Hvide Sande wind data is measured with an Ultrasonic anemometer (WindObserver65) and data sets consist of wind speed, direction, atmospheric pressure, temperature and max gust.

The wind gauge sits on top of a harbour control tower within the town of Hvide Sande. Wind measurements might be affected by turbulent winds due to obstacles such as harbour buildings and terrain. Furthermore, three windmills are located on the beach only 1 kilometre away in the direction of W to NW.

Despite the obvious obstacles when using wind data from Hvide Sande, these have been chosen for further analysis in this report as, based on distance from study site, they are considered to best represent the coastal stretch at Skodbjerge. The wind data from Blaavand is analysed in detail in the Master Thesis written by Magnus Bank Krog, University of Copenhagen (Krogh, 2019), which dealt with a coastal stretch just north of the study area of this report.

Figure 4-1: Study area (red square) and available wind measurements.

4.2.1 Data validity

The quality of the Hvide Sande data is checked before they are included in the database, but missing data are not corrected or filled in by interpolation. A time series of wind data from Hvide Sande between 30-03-2006 and 15-07-2019 have been examined in this report. For the data set, "NoData"-values are found for roughly 3.5 % of the whole period (≈ 172.5 days). Naturally, the missing data is not evenly distributed throughout the period. Further elaboration on this will be made in the description of methodological approach.

Period	Length (days)	Length (hours)	From	To
1	777	18648	30-03-2006	15-05-2008
2	317	7608	16-05-2008	29-03-2009
3	523	12552	30-03-2009	04-09-2010
4	466	11184	05-09-2010	15-12-2011
5	332	7968	16-12-2011	12-11-2012
6	394	9456	13-11-2012	12-12-2013
7	492	11808	13-12-2013	19-04-2015
8	357	8568	20-04-2015	11-04-2016
9	372	8928	12-04-2016	19-04-2017
10	356	8544	20-04-2017	11-04-2018
11	460	11040	12-04-2018	16-07-2019

Table 4-2. The periods divided by start and end. Start represents the first day after previous LiDAR was finished while end represents the last surveying day of the following LiDAR. Lengths of periods are described as days and hours between DEM sensing's.

4.3 Orthophotos

Regional and national orthophotos from 1954, 1995, 1999, 2002 and each year in the period from 2004 to 2019 are available for the stretch and are presented in Appendix A. These are primarily included if required to determine distinct uncertainties when analysing the DTMs. Here additional orthophotos from LiDAR scans between 2012 and 2019 are also reviewed but will not be included in the report.

4.4 Drone imagery

On several field trips to the area, drone videos and imagery have been collected. The available videos are from 24 May 2016, 24 October 2017, 12 June 2018, 28 March 2019, and 23 July 2019.

The imagery from 28 March 2019 and 23 July 2019 were provided for the current report, and are the only ones utilized. Drone videos and images have only been used for visual analyses of the study area. The drone used was a DJI Mavic Pro (28 March) and a DJI Phantom 4 Pro (23 July).

5. Methods

5.1 Division of study period

LiDAR data is the primary data sources in this report. The data set has therefore been used for periodical divisions of the overall study period. The periodical division is presented as period 1, 2, 3 etc. together with the length of the given period in hours and days, as well as the time period it covers in Table 4-2. Notice that the dates dividing the periods are the same as for the LiDAR scans. One main goal of the report is to describe the changes between LiDAR measurements and quantify them over time and it is therefore reasonable to divide the study period into shorter periods corresponding to the periods between the LiDAR scans.

5.2 Difference mapping

Difference maps are made in ArcMap using the tool "Minus" (spatial analyst). The tool subtracts one raster layer from another. The results are raster layer outputs representing the difference between data sets on raster cell level, which in this case illustrates any elevation change. The older of the two is used for subtraction of the newer, which means positive changes are elevation increase, and negative changes are a decrease in elevation.

Before spatial analysis can be initiated, the boundaries of the study area must be defined. In order to minimize time consumption for difference mapping, the original LiDAR mosaics (From Lodbjerg to Nymindegab) are "clipped" to a predefined rectangular polygon defining the study area extent. The rectangle must be large enough to include the full cross-shore extent of all the LiDAR scans. By using the iterator tool in the Model Builder (Figure 5-1), the clipping function can be automated, and all local LiDAR-clips will be collated in the same location. The individual year-to-year difference mappings were made manually for each period.

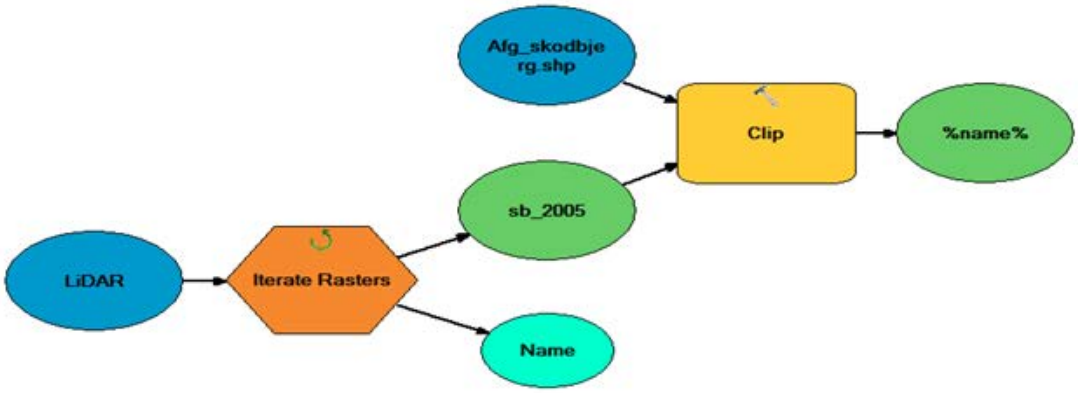

Figure 5-1. Model Builder created in ArcMap showing the work flow for clipping of the original LiDAR mosaics to a polygon defining the extend of the study area.

Using the Minus-tool the output raster cell grid will be the same as the coarsest grid used for inputs, if not otherwise defined in the environmental settings. E.g. when 2006 (1 m x 1 m) is subtracted from 2008 (1.6 m x 1.6 m) the output raster layer will have a 1.6 m x 1.6 m cell size. The Minus-tool automatically resamples the finest raster layer grid into the coarsest cell grid. The resampling method can be determined in the environmental setting of the tool, but in this case the default method "nearest neighbour" is used for resampling. This will increase uncertainties and distortion in the difference mappings, but in this case it has been evaluated as best approach, as resampling of all data sets could increase uncertainties, and the primary goal is to visualise trends in erosion/accumulation.

Two types of difference mappings are included in the report. Difference mapping is presented for the changes between LiDAR, which means that year-to-year changes are detectable. All maps are found in Figure 6-2 and Figure 6-3. In addition, the accumulated change in the period is presented for the overall period as a difference map between 2006 and 2019.

5.3 Division of stretches

The dune face is known to retreat in the study area, but whether or not this retreat is compensated by accumulation of sediment inland of the dune crest is not clear. In order to describe the sedimentary budget in the area affected by aeolian processes, exchange of sediment between stoss and lee side of the dune crest must be analysed. The study area is divided into two cross-shore boxes (seaward and landward), which represent the dune stoss side and the area leeward of the dune crest. The basis for the boxes are three distinct boundaries:

- The boundary between the seaward box and landward box is based on the difference mapping between 2006 and 2019. This difference mapping showed a distinct separation between a seaward area of erosion and a landward area of accumulation. This line of separation was found to reflect the position of the dune crest in 2019. This boundary was selected to separate landward and seaward boxes, as it separated erosion and accumulation, while still symbolizing the 2019 dune crest position. A polyline feature was computed in ArcMap by extracting the 0 m contour in the difference map 2006-2019 ("contour" tool). The line reflected was a very fine line, but as it was to be used in raster analysis later, the high degree of detail was unwanted and it was then simplified by a factor of 100 m.
- Morphologically, the seaward boundary would be somewhere on the beach, roughly where the dune toe can be identified, but since this is difficult to compute, a more practical approach was implemented. The planimetric position of the 4 m contour from 2006 was set as a fixed boundary. This ensured a contour well above any water levels in the period while also including the safety level in the analysis (4.5 m).
- The inland boundary of the landward box represents the maximum extent of aeolian deposition during the study period. A Normalized Difference Vegetation Index (NDVI) analysis of the 2018 orthophoto, established the extent to which the aeolian deposition could be traced in the vegetation. This resulted in an inland demarcation enclosing the potential maximum inland extent of aeolian deposition for 2018 and the line feature was simplified by a factor of 100. As the 2018 orthophoto is the only one available with the near infrared band, manually correction had to be done to the remaining years. The manual correction was made by first visually identifying areas with deposition inland of the 2018 demarcation and then extending the line feature.

After dividing the stretch into a landward and a seaward box, a further division into five alongshore sections were made (Figure 5-2). This resulted in creation of 10 boxes for volume analysis and evaluation of sedimentary budget. The sections are numbered 1 to 5 from north to south, while cross-shore boxes will be referred to as seaward and landward boxes. Accordingly, the northernmost landward box is named: Landward box section 1 or L1 in short.

When performing data analysis in these sections and boxes, it is necessary to take the width of the individual scans into account. The 2013 scan is e.g. much narrower than all other scans, which means that manual corrections were required for the volume analysis, in order to include cells outside of the 2013 scan.

Figure 5-2: The boxes used for volume analysis in study area of Skodbjerge. Numbering is from north to south with a prefix indicating the overall box. For example, S1 is the northernmost seaward box.

5.4 Volume calculations

To quantify the aeolian changes in the dunes over time, different volumetric analysis approaches were tested. Volume calculations are based on the boxes as defined in section 5.3.

Two methods were tested for volume calculations:

1. Volume calculation using the "surface volume" tool (3D analyst toolbox) in ArcMap.

The surface volume tool calculates a 3D volume between a surface and a certain reference level. It is not possible to limit the calculation to a defined area, and the raster layers must therefore be split into smaller areas for volume calculations. All LiDARs are clipped to the extent of each of the individual boxes presented in Figure 5-2, as we are interested in the volume development in each of the defined boxes. The surface volume analysis is carried through for each new raster layer from the reference level 0 m. As the process of first clipping the LiDAR and then calculating the volume on all included LiDAR data sets requires 280 manual operations in ArcMap, the process is time consuming. The process was automated using ArcMap desktops Model Builder tool, which gave a more effective workflow - the model is represented in Figure 5-3. The result was 140 text files (10 boxes x 14 rasters) which were imported into Excel for analysis.

When working with iterators in Model Builder, using the %name% function, it was ensured that the LiDAR name (here the year) was present in the text file name and that the "box name" (e.g. S1) was included as extension in the file names as well. As both year and box were included in file names, the basis on which the volumes were calculated was highlighted, and the extent of each raster layer was known, as the clipped files were saved. Backtracking for error tracing was relatively simple when using this method.

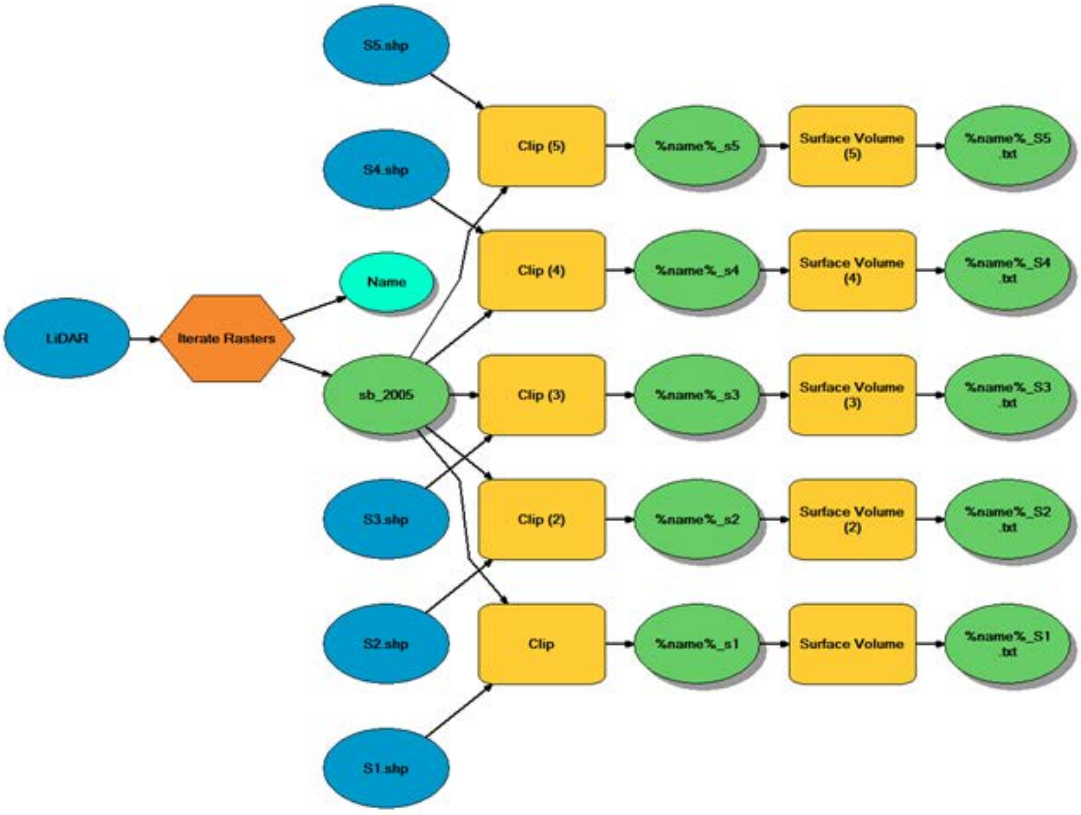

Figure 5-3. Model Builder created in ArcMap showing the work flow for volume analysis of the LiDAR scans using the surface volume tool.

2. Volume calculation using the "Zonal statistics as table" tool (Spatial analyst) in Arcmap.

The second approach is more simplistic, and based on a tool, which can handle polygon features as boundary conditions. The Zonal statistic tool summarizes, max, min, sum, area etc. of the raster cells within a

predefined polygon and output data set is an “info table” which is converted to text by the “table to table” conversion tool for easier import to Excel (Figure 5-4). When using a feature dataset as boundary, an internal vector-to-raster conversion is applied to the zonal input. If no extent is defined in the environmental settings, the input features define the extent of the analysis and the raster conversion is made to the input boundary polygon. It can be argued that resampling the original datasets to equal raster resolution would have been appropriate, but this extra step would result in loss of information in the conversion steps. The polygon feature consists of multiple features (not overlapping) and the zonal statistics tool summarizes for all polygons and the result is only 14 info tables. These must be converted. This makes the process much simpler and much less time consuming and the required data storing space is significantly lower compared to the clip method.

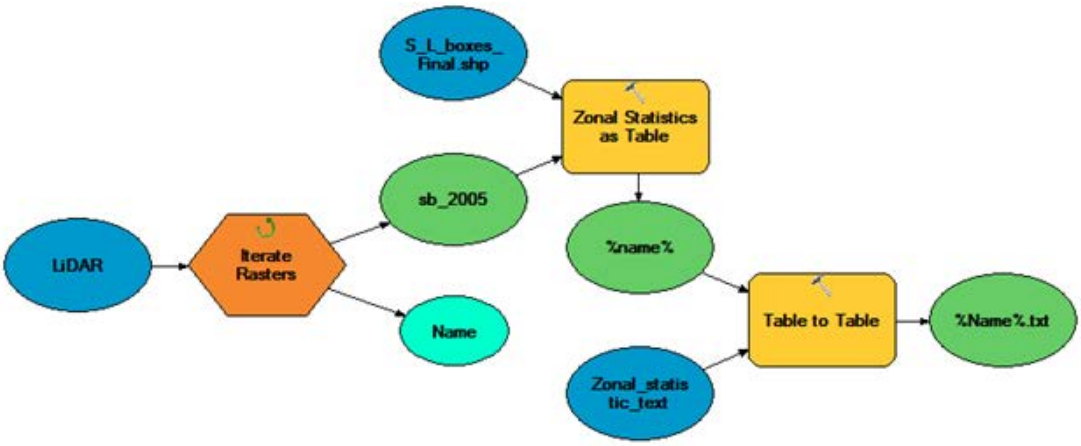

Figure 5-4: The zonal statistics to table method described from a model made in ArcMap Desktops Model Builder module.

5.5 Safety level

The safety level of the dunes is set to be 40 m of width at the 4.5 m contour. Therefore, the analysis of the changes must reflect the 4.5 m contour.

5.5.1 Dune width at 4.5 m

The dune width is determined across the dune at perpendicular station lines from seaward 4.5 m contour to landward 4.5 m contour.

All LIDAR scans must be converted into contour layers containing the 4.5 m contour (“Contour” tool). All new contour features must have an attribute file containing the year, which they represent. All contour layers are then merged into one main layer (“Merge” tool). A selection based on contour=4.5 m and a removal of all lines <2000 m are conducted to maintain primary inner/outer contours representing the safety level. The 4.5 m contour is new in one layer with an attribute giving the year from which it dates.

A straight baseline feature is created alongshore and placed seaward of the contour layer. From the baseline, perpendicular lines are created for every 10 meter. These station lines are numbered from 0 in north with a linear increase of 10 towards the south until reaching the ultimate line, number 3660.

The intersection between station lines and all 4.5 m contours for all years were found using the “Intersect”. The output was a multipoint feature. This was then edited in advanced editing setting and all features were “exploded” into singular points. The multipoint feature was converted to a point layer (“Feature to point” tool) and imported to the “generate near table” tool together with the baseline. The output was a table file containing the planimetric distance from each intersection point to the baseline. Since station lines are created perpendicular to the linear baseline, the setting “shortest path” ensures that the output distance between point and baseline line is at the station line end on the baseline.

As the 4.5 m contour is not straight and also exists inland of the dune leeside (as seen in the profile Figure 1-2), intersections are found more than just twice on the same station line. Values must therefore be sorted so only the two smallest values (distance from baseline) for each station line each year exist in the dataset. This is performed using a python script.

This sorting method is solid and performs well, but some errors appear when the seaward 4.5 m contour exists multiple times on the same station line, and the dune width shows up as unnaturally narrow. This is simply due to the natural curvature in blowouts and sometimes due to incipient dunes at the dune toe. Manual detection of these features is still necessary and correction of 72 out of 4392 widths was performed. Furthermore, there are examples of the LIDARs scans simply being too narrow to include the inland 4.5 m contour (as seen in 2013). Here the landward 4.5 m contour is assumed.

5.5.2 Volume above 4.5 m and planimetric area at 4.5 m

Clipping and surface volume approach is introduced for this analysis as the reference level for volume and area calculations can be set manually, in this case at 4.5 m.

Instead of analysing the singular boxes, we now want to analyse across both seaward and landward boxes, therefore LiDAR scans were clipped to the sections (1 to 5 with 1 being the northernmost section). Then the surface volume tool was applied for all new raster layers with reference level set to 4.5 m. No resampling or environmental changes were made.

Results are given as area in 2D (planimetric), area in 3D (surface area of volume above 4.5 m) and volume (volume above the reference plane).

The volumes were normalized by dividing with the length of the individual section. The planimetric area was also divided by the length of each section and the result could be regarded as the average width along the stretch.

There will be differences along the boundary between sections due to differences in cell size and the use of the clipping and surface volume approach, but most of the errors are irrelevant when analysing a contour which moves in time. The boundaries are therefore only fixed in terms of sectional extent, but otherwise free to move, and the area is therefore expected to change as the morphology changes. When using this method, the 4.5 m contour is set as boundary condition, which means boundaries are not fixed in space and time, only in elevation. The results do not show any actual displacements.

5.6 Relation between wind climate and aeolian transport

One of the hypotheses was that the wind climate is reflected in the amount of sediment eroded and accumulated. By estimating the threshold fluid velocity, the number of hours (in each period) above this threshold can be found for all on- and alongshore wind directions which can then be compared to the actual volume change.

The coastal orientation at Skodbjerge is ≈355°, and in order to limit the wind data to measures only reflecting directions from which sediment transport could be on- or alongshore, the overall data set was limited to contain only winds between 170° and 360°. 5 degrees was included on both sides of the coastal orientation to reflect differentiated coastal orientation along the stretch. Afterwards, the data set was resampled (see description on how in following chapter 5.6.2) into closed hourly bins. Holes in the data set could not be considered errors as several measurements were sorted out.

By plotting the number of hours above the threshold fluid velocity in each period against the actual erosion (m^3) or accumulation (m^3) a very simple correlation test was performed.

5.6.1 Critical threshold fluid velocity

Mean grain sizes from 6 profiles, few kilometres north of the current study area, was presented in (Krogh, 2019). In the report, 17 sediment samples have been included for definition of a mean grain size, which was used as input parameter in a transport model. 8 samples are from the dune face (2 samples from four different profiles), 6 samples are from one blowout section, and the remaining 3 samples are from a dune ramp. Therefore, there was a high spread between the spots from which the samples were taken, but this gave a good indication of the native grain sizes on the stretch. Sediment samples were taken with a soil-sampling ring (Ø60mm H35mm) and a trowel.

The sediment size used for estimation of threshold fluid velocity was 282 um. This value was derived from (Krogh, 2019) where mean sediment grain size across and along the foredunes was found between 282 um to 336 um. The overall mean was 324 um.

Lowest mean grain size was used for estimations of critical threshold fluid velocity in order to describe the point at which sediment movement was initiated. The sampling took place 1-5 km north of the study area in this report, but the samples are expected to represent this study area, too.

Calculation of the threshold fluid velocity in Hvide Sande (z = 25 m) was 8.94 m/s and 8.95 m/s when using the two approaches described in section 3.5 and the difference is in this case negligible. Parameters used are presented in Table 5-1.

A	Air density	Gravitational acceleration	Material density (quartz)	Davg	K
0.1	1.25 kg/m³	9.81 m/s²	2650 kg/m³	0.000282 m	Davg/30

Table 5-1: Parameters used for calculation of the threshold fluid velocity.

5.6.2 Resampling of wind data

A test was made to check for missing data between each LiDAR scan and as seen in Table 5-2, periods 2, 6 and 8 are most affected by missing wind data – note that the table describes the original dataset without resampling. For further analyses the data have been resampled in order to standardize data for a test between threshold fluid velocity and hours above the critical threshold fluid velocity.

Data setup	Hours in period	Hours in dataset	Missing data (Hours of period)	Missing data (% of period)
Period 1	18648	18359.0	289.0	1.5
Period 2	7608	6776.8	831.2	10.9
Period 3	12552	12297.2	254.8	2.0
Period 4	11184	11110.5	73.5	0.7
Period 5	7968	7945.2	22.8	0.3
Period 6	9456	8828.5	627.5	6.6
Period 7	11808	11797.8	10.2	0.1
Period 8	8568	7016.0	1552.0	18.1
Period 9	8928	8920.0	8.0	0.1
Period 10	8544	8442.8	101.2	1.2
Period 11	11040	10671.7	368.3	3.3

Table 5-2. Amount of missing data in each period presented as number of missing hours of the total data set and percentage of the total data set. Based on the original data without manipulation.

A resampling of the data was conducted on the basis of closed hourly averages of available data. If a full hour (e.g. between 08:00 and 09:00) had no data measurements, this time step was excluded from the data set. If there was one or more measured values in a time step, it was included based on the average of available measures in the given time step.

The resulting re-sampled data set was tested against the original, based on the difference between the average wind speeds in the overall data set. This test revealed a 0.0016 m/s difference and with such a small difference, the resampled data is acceptable for the analysis.

It is necessary to stress that wind speed is measured at approximately 25 m height (relative to DVR90). If wind speed were to be related to the wind experienced on the beach, a transformation of the measurements to the relative height at the beach with respect to the logarithmic wind profile would be necessary. This was not performed as there are no in-situ wind measurements to correlate modified wind velocities to. Instead, the critical threshold fluid velocity has been related to the height of 25 m.

6. Results

6.1 Difference mapping

Difference mappings are presented at the end of section 6.1.1 (Figure 6-2 and Figure 6-3). The change between 2006 and 2019 is presented together with the changes in all 11 periods. The reader will notice that the legend does not represent equidistant intervals in the elevation change. This current legend was basically made on the basis of best fit found by trial and error. Changes between -0.1 m and 0.1 m has no colour indication. This decision was made to make sure that only "significant" elevation changes were displayed, while potential scattering, distortion or vegetation change induced elevation changes were filtered out. The difference maps show some alongshore features at the back of the foredune. These indicate the ridge of a dune reinforcement made in 1994 that has created a plateau at the back of the foredune and the alongshore features are shown to be accumulations of sediment along the leeside of the dune reinforcement. The dune reinforcement is clearly visible in the orthophotos from 1995 in Appendix A as bare sand surfaces along sections 1, 2 and 3.

6.1.1 Temporal changes in dune area

6.1.1.1 Section 1

The overall temporal change in section 1 from 2006 to 2019 indicates dominating erosion in S1 and accumulation in L1. Several blowouts are present along the stretch of dune and erosion primarily takes place in the deflation basins of these blowouts and in the southern end of S1. Landward of the deflation basin, in L1, accumulation of sediment dominates with hotspot accumulation in the depositional lobes of the blowouts. However, along the entire stretch of section 1, sediment accumulates at the back of the dune and at the plateau landward of the foredune ridge (dune reinforcement). The amount of accumulated sediment decreases with distance from the deflation basins of blowouts. Section 1 is the only section where the beach area, seaward of the seaward box, has been subject to accumulation along the entire stretch of the section, when analysing the elevation change from 2006 to 2019.

Analysis of difference maps of the elevation change in section 1 demonstrated a temporal variation in the annual elevation change. From 2006-2008 the outer part of S1 was exposed to erosion along the entire stretch and the inner part of S1 was subject to accumulation with exception of a few blowouts in the northern part. This area of accumulation in the inner part of S1 is found to correspond to the area leeward of the dune crest location in 2008. The difference map 2006-2008 shows alongshore features of deposition in L1 at the back of the dune, which connects depositional lobes of individual blowouts. This was caused by the dune reinforcement carried out in 1994, which affects the deposition of sediment in the dune area. In general L1 shows accumulation in most of the dunes section, while there is close to no changes in the inland section of L1.

The difference map 2008-2009 showed that the outer part of S1 has been subject to accumulation and that the inner part of S1 has also seen accumulation, which was the exact opposite as the change seen in the previous year. The primary erosion is seen in the deflation basins of blowouts. The elevation change of 2008-2009 stands out by having only very little accumulation of sediment in depositional lobes and the accumulation is low compared to the other periods. From 2009 to 2010 the same changes are seen but with less accumulation leeward of the foredune ridge.

The difference map 2010 to 2011 shows comparable development to period 1 but with a slight increase in the erosion of the inner part of S1, and with increase in accumulation in depositional lobes in the southern part of section 1.

From 2011 to 2012 a possible undulation is seen to decrease the beach volume along sections 3, 2 and into the southern part of section 1. This is also visible in the 2012 orthophoto as a scarping on the beach

moving almost diagonal across the beach in section 3 into the dune face of section 2. This resulted in slight acute erosion of the dune face in the southern part of S1. Accumulation is present along the full stretch of L1 with hotspots in depositional lobes.

From 2012 to 2013 the southernmost part of S1 experienced remarkable larger erosion than in other years. This is a result of acute erosion. S1 shows erosion along the whole stretch for the first time. Accumulation in L1 primarily takes place in the northern part of the section. Furthermore, it is worth noticing that the deflation basin of the largest blowout extends into the area of the landward box where depositional lobes were previously located. Whether this is a result of the northern blowouts extending inland is difficult to tell from orthophotos, but as it seen again in period 7 to 11, it is likely to be the result of landward movement of the deflation basin and the depositional lobe. The following years from 2013-2015 (period 7) accumulation is present in the outer part of S1, especially where acute erosion took place from 2012 to 2013. Deflation basins continue to erode and move inland into L1.

In period 9 accumulation of sediment is mainly taking place in depositional lobes of blowouts, whereas sediment in the previous periods has accumulated leeward of the entire dune crest. Especially the difference maps of 2017-2018 (period 10) and 2018-2019 (period 11) show large accumulations of sediment along the entire leeside of the dune crest. S1 also shows larger spots without elevation changes (changes from -0.1 m to 0.1 m). Furthermore, the difference maps of 2017-2018 and 2018-2019 show accumulation in the outer part of the seaward box and in areas, which would be expected to be deflation basins.

6.1.1.2 Section 2

The overall temporal change in section 2 from 2006 to 2019 is that S2 is dominated by erosion and L2 is dominated by accumulation. The amount of accumulated sediment decreases as the distance from S2 increases. At the back of the dune there is an alongshore feature of accumulated sediment, which was caused by the dune reinforcement carried out in 1994. The extent of the sheet of accumulated sediment is significantly narrower than those found in all other sections. There is only one small blowout present at this stretch of dune, which means that the dune face is relatively regular with almost no deflation basins or depositional lobes. Accumulation of sediment takes place at the dune leeside along the entire stretch of L2. The largest amount of sediment accumulated in L2 is in the depositional lobe of the only blowout present.

There is a temporal variation in elevation change of S2. For most of the study period the elevation change differs within the box, as a result of the dune crest being located in the middle of the seaward box. This means that an outer and an inner part of the seaward box appears, representing the dune face and the area leeward of the dune crest, respectively. The dune face is dominated by erosion in 2006-2008, 2011-2012, 2012-2013, and 2015-2016. In 2009-2010, 2013-2015, 2016-2017, 2017-2018, and in 2018-2019 the dune face is dominated by accumulation of sediment.

One of the most significant changes in section 2 is in period 5 and 6 (2011-2012 and 2012-2013). As mentioned for section 1, a decrease in the beach volume in period 5 leads to acute erosion, and this is most pronounced in section 2. The decrease in beach volume might have induced the extensive dune face retreat seen in period 6. The dune crest is still visible in the spring orthophoto from 2013, but the LiDAR scan from 2013 was not performed until mid-December and the dune face has eroded after the orthophoto was taken. In the 2014 orthophoto, the dune crest has retreated to the boundary between the seaward and landward boxes. The dune crest position from 2014 has remained almost in the same position until the latest orthophoto from 2019.

From 2013 to 2017 the only accumulation of sediment in the landward box (L2) is in the depositional lobe of the small blowout. Almost no sediment accumulates at the leeside of the dune, which is different from the rest of the study period in which sediment accumulates along the entire leeside of the dune.

6.1.1.3 Section 3

The overall temporal change in section 3 from 2006 to 2019 is that the seaward box (S3) is dominated by erosion and the landward box (L3) is dominated by accumulation. The largest accumulation of sediment in L3 is found in the depositional lobes of blowouts. However, accumulation of sediment takes place at the leeside of the dune along the entire stretch (Figure 6-1). In the southern part of the area an alongshore feature of accumulated sediment is found. This is caused by a previously performed dune reinforcement. It is to be noticed that the blowouts are large and located very close to each other, causing the depositional lobes to merge and create a blanket of accumulated sediment at the leeside of the foredune. The top and vegetated part of the dunes along 2/3 of section 3 has migrated significantly inland over a sort of plateau. This is clearly demonstrated in Figure 6-1. Seaward of the dunes a sharply defined ridge with pebble and gravel paving represents the dune face. Although this ridge looks man-made there are no indications from historical sources (neither in reports nor in orthophotos) that it should be man-made, and it is therefore considered a morphological feature. At this point there is little knowledge of the formation and development of the ridge.

Figure 6-1: Drone footage from the 28t March 2019. Red lines mark the section boundaries for section 3.

The dune face of section 3 has been exposed to erosion in 2006-2008, 2010-2011, 2012-2013 and 2015-2016. However, spatial and temporal variations in the changes of the dune face of section 3 are found during the study period.

In 2017-2018 and 2018-2019 accumulation takes place along the entire leeside of the foredune compared to other years where accumulation is more or less restricted to the depositional lobes of blowouts. The largest accumulation of sediment in L3 also occurs in 2017-2018 and 2018-2019 when the deposition increases in depositional lobes of blowouts while accumulations along the leeside of the dune are more widespread than in previous periods.

6.1.1.4 Section 4

The overall temporal change in section 4 from 2006 to 2019 is that the seaward box (S4) is dominated by erosion and the landward box (L4) is dominated by accumulation. The largest accumulation of sediment in L4 is found in the depositional lobes of blowouts. The largest erosion in S4 is in the deflation basins and along the dune face. In the centre of section 4 several blowouts have merged and created a large blowout area. This means that the depositional lobes have also merged and created a blanket of accumulated sediment.

The difference maps of 2006-2008 and 2017-2018 show accumulation of sediment along the entire leeside of the foredune, whereas the other difference maps show deposition primarily in the depositional lobe of blowouts. However, all difference maps show the largest accumulation of sediment in the depositional lobes of blowouts. This is similar to the development seen in sections 3 and 5.

The dune crest is relatively stable between 2006 and 2019 in contrast to sections 1, 2 and 3. However, between 2007 and 2008 there is erosion of foredune notches, and between 2010 and 2012 there is acute erosion along the full stretch of section 4. From 2012 to 2019 no acute erosion seems to be taking place at the dune toe, but the blowouts increase in width and size due to aeolian transport.

The difference map of 2008-2009 shows the smallest accumulation of sediment. The elevation change in the depositional lobes is small and the accumulation is primarily found in the depositional lobe of the largest blowouts. The largest accumulation of sediment in depositional lobes of blowouts is found in the difference map 2017-2018 and 2018-2019.

In 2009-2010 erosion in the deflation basin starts to evolve into the landward box (L4). This continues for the annual elevation change for the rest of the study period. However, when looking at the difference map 2006-2019, for the overall study period it is found that erosion in the deflation basins of blowouts stays within the seaward box (S4) except for one blowout in the centre of L4. This is comparable to the development, which was seen in section 1. Section 5 shows some similarities, but more sporadic.

In 2006-2008, 2010-2011, 2011-2012 and 2017-2018 there is a distinct boundary between an area of accumulation and an area of erosion in the seaward box (S4). The difference is that in 2006-2008 and 2010-2011 the outer part is exposed to erosion while the outer part in 2011-2012 and 2017-2018 is exposed to accumulation.

6.1.1.5 Section 5

The overall temporal change in section 5 from 2006 to 2019 is that the seaward box (S5) is dominated by erosion and the landward box (L5) is dominated by accumulation. Large blowouts are present in this section with erosion in the deflation basins and accumulation in the depositional lobes. The largest erosion is found along the dune face and in deflation basins of blowouts. The largest accumulation of sediment is found in depositional lobes of blowouts, but relatively large accumulations are also found inland of the dune crest. In the southernmost part of section 5 a deflation basin is present landward of the dune crest detached from the dune face. The most landward facing part of this deflation basin has been exposed to erosion during the study period from 2006-2019, while sediment has accumulated in the area between this detached deflation basin and the dune face. Furthermore, a gravel road between a parking area and the beach creates an elongated feature in the difference maps, which shows annual changes of erosion and accumulation.

In 2006-2008, 2010-2011, 2017-2018 and 2018-2019 accumulation has taken place at the entire leeside of the foredune, whereas the rest of the study period accumulation has primarily taken place in depositional lobes of blowouts.

In 2006-2008 large accumulations of sediment are found in depositional lobes of blowouts in the southern part of section 5. The difference map 2016-2017 shows that almost no sediment has accumulated at the leeside of the foredune with exception of depositional lobes of blowouts where sediment accumulates leeward of deflation basins.

The difference map of 2016-2017 shows erosion of the entire seaward box (S5). 2010-2011 and 2012-2013 are also dominated by erosion, whereas the elevation changes during the remaining years are more variable within the seaward box.

The seaward box shows a distinct boundary between an outer and an inner part of the box dominated by either erosion or accumulation. This boundary in the seaward box represents the morphology of the

foredune, which retreats during the study period. It is found that there are annual changes as to whether the outer part of the seaward box is dominated by erosion and the inner part dominated by accumulation or the opposite.

From the 2010-2011 difference map and onwards the deflation basins evolve from the seaward box (S5) into the landward box (L5). However, this erosional feature is not found in the 2006-2019 difference map due to accumulation at the beginning of the study period.

6.1.1.6 Summary of temporal changes

Some of the temporal changes observed during the study period apply to all five sections while others only apply to some of the sections.

There are large temporal variations in the development of the outer part of the seaward boxes. It is found that for all sections, accumulation dominates in period 3, 5, 10 and 11, whereas this area has been dominated by erosion during other years, namely periods 1, 6 and 9. The remaining years of the study period the temporal changes of the outer part of the seaward boxes vary spatially.

It is found that in some specific subareas of the study area there is a clear temporal variation in accumulation and erosion. If one of these subareas is exposed to erosion one year, the following year the exact same area is exposed to accumulation. An example of this is the outer part of the seaward box in section 3 (S3) where erosion took place between from 2009 -2010 and the following year 2010-2011 the difference map shows accumulation in the exact same area.

In periods 1, 4 and 10 accumulation has taken place landward of the dune crest along the whole stretch. In the remaining periods sediment primarily accumulates in depositional lobes in the leeside of deflation basins of blowouts. Especially in period 9 almost no sediment accumulated in the landward box along the leeside of the foredune, the only accumulation of sediment is in depositional lobes of blowouts.

From 2006-2008 and 2017-2018 accumulation takes place in the lee side of the entire stretch of dune and is not restricted to the depositional lobes of blowouts, which is where the sediment is primarily deposited the remaining years.

During all the years accumulations have taken place in the depositional lobes of blowouts. Difference maps of 2008-2009, 2011-2012 and 2012-2013 show smaller accumulation in depositional lobes than the rest of the study period, however accumulation is still present, especially in section 4 where the largest accumulation takes place during these years.

The deflation basins of blowouts develop through the study period. All difference maps show relatively large annual erosion in deflation basins. The only map that shows smaller erosion than the rest is the difference map from 2008-2009.

Acute erosional events are found to have significant impacts on the dune face at several occasions. Especially during the period from 2011-2013 section 1, 2 and 3 have been exposed to large erosion of the dune face.

When looking at the area below the 4 m contour it is found that there is a large temporal variation in the elevation change of the beach. This area is outside of the defined boxes and therefore the beach area seaward of the 4 m contour in 2006 will not be analysed further.

Besides the described natural changes of the dune area there are some anthropogenic impacts which can be seen from the difference maps, such as dune reinforcement, walking paths, gravel roads and a parking area. This affects the aeolian processes and can lead to features of accumulation and erosion with an unnatural appearance in the difference maps.

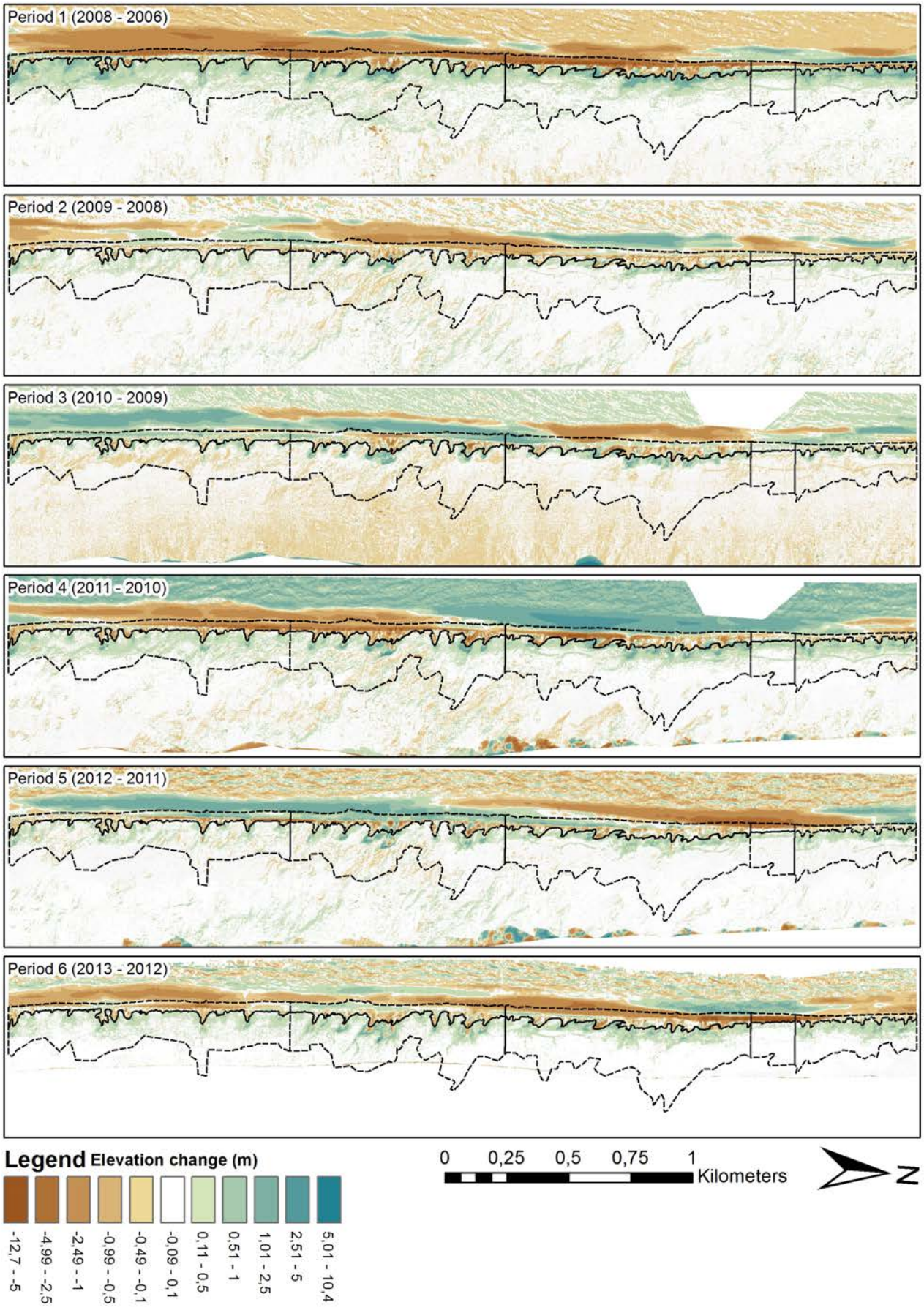

Figure 6-2: Difference maps for periods 1 to 6. Period for each difference map is indicated in upper left corner of each difference map.

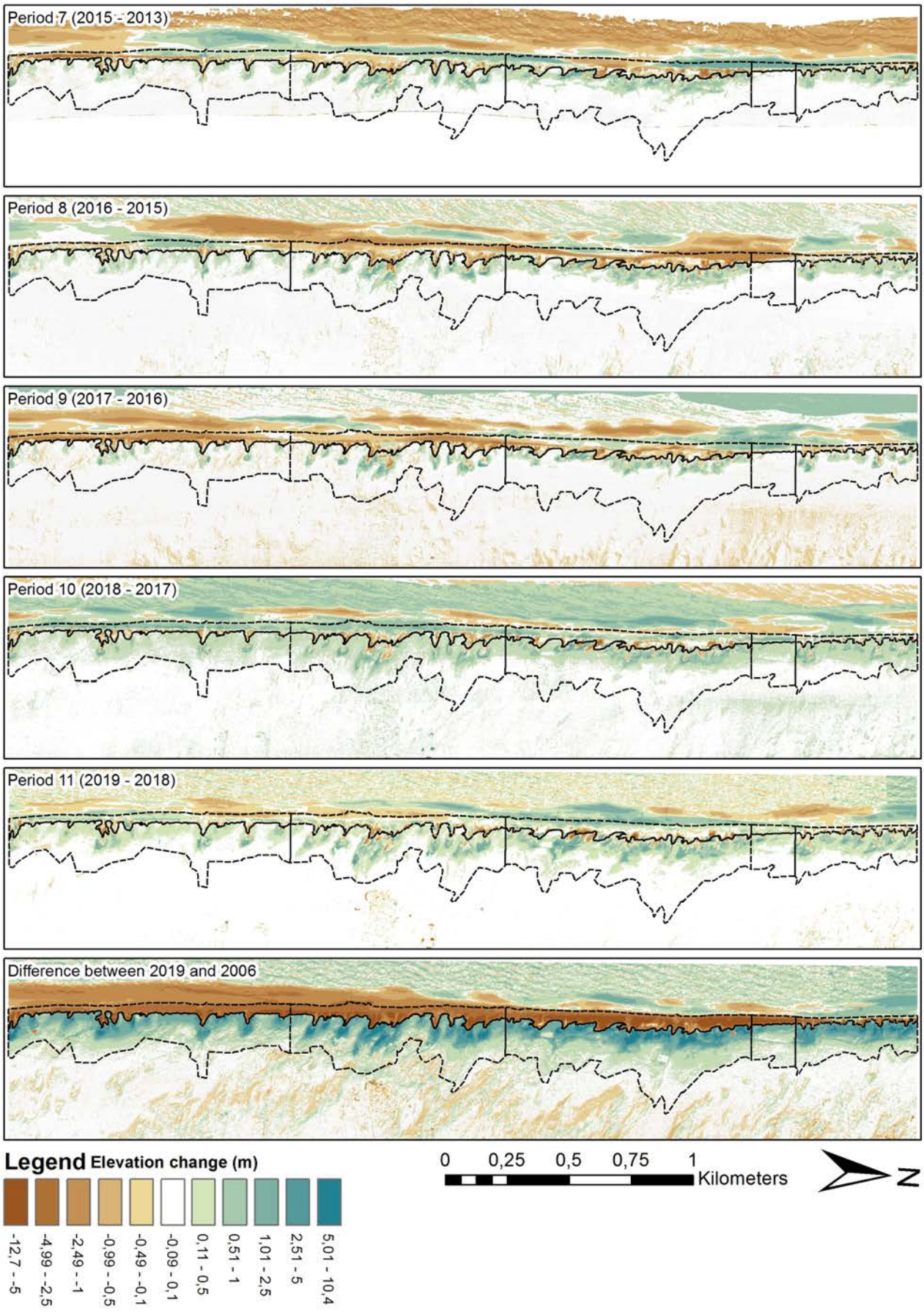

Figure 6-3: Difference maps for periods 7 to 11 and difference map showing the change between 2006 and 2019. Period for each difference map is indicated in upper left corner of each difference map.

6.1.2 Spatial variation in elevation changes of the dune area

There are alongshore variations in the elevation changes of the area during the study period (Figure 6-2 and Figure 6-3) and total change have been illustrated with 3D-models in Figure 6-4. Blowouts are very distinctive morphological features in the dune area and a spatial variation is found in the development and presence of blowouts. The alongshore variations in numbers and sizes of blowouts affect the dune development during the study period, since these are morphological features, which highly affect the sediment transport in the dune area causing erosion and accumulation. Sections 3 and 4 are more affected by blowout evolution causing changes of the dune compared to the other sections. In sections 3 and 4 the spacing between blowouts is shorter than in the rest of the study area and some blowouts have merged into a large coalesced blowout. Relative large blowouts are present in section 5 as well, but these blowouts are more separate than blowouts in other sections and their depositional lobes do not extend as far inland as others do. In section 2 there is only one small blowout and therefore this section has a more regular dune face. In section 1, many blowouts are present in the dune, but these blowouts are small compared to blowouts in sections 3-5.

Besides a spatial variation in numbers and sizes of blowouts, it is found that the orientation of the blowouts vary along the study area. In sections 1 and 5 the orientation is close to coast normal while the blowouts in section 4 have more oblique angles with an orientation towards southeast. The orientation of blowouts in section 3 are relatively varied whereas blowouts in sections 1, 4, and 5 are more unidirectional. Section 2 has only one small blowout and its orientation is difficult to determine.

Accumulation of sediment dominates the landward boxes and there are some spatial variations in the study area which are mainly initiated by the presence of blowouts. The difference maps show that the amount of sediment accumulated landward of the dune crest is largest where the numbers and sizes of blowouts are large, such as sections 3 and 4. In comparison section 2, with the least blowouts, experiences the smallest accumulation of sediment leeward of the dune crest during the study period. In sections 4 and 5 accumulation in the landward box is mainly restricted to the depositional lobes leeward of the deflation basins of blowouts. In sections 1 and 3 deposition in the landward section is fairly evenly distributed along the stretch. However, the largest accumulation of sediment is still located in the depositional lobes of blowouts. In section 2, accumulation in the landward box takes place along the entire stretch of dune with the only exception being a small depositional lobe with increased accumulation.

Generally, the seaward boxes are dominated by erosion but spatial variations are found along the study area. Section 1 has the narrowest seaward box, which is also the box in which the erosion within the seaward box is the lowest. Parts of this box have even been exposed to accumulation of sediment during the study period. The most intensive erosion occurs in sections 3 and 4 in the upper part of the dune, the dune face, and deflation basins of blowouts. In section 2, erosion is restricted to the upper part of the dune and the dune face but this is also the area with the most even and distinct dune crest. In section 5 the difference maps show that a deflation basin is located in the landward box detached from the dune face.

In the maps of annual elevation changes spatial variations in the beach section seaward of the seaward box are found. These changes are not accounted for as they are outside of the defined boxes, but they can also influence the dynamics, sediment transport and dune morphology.

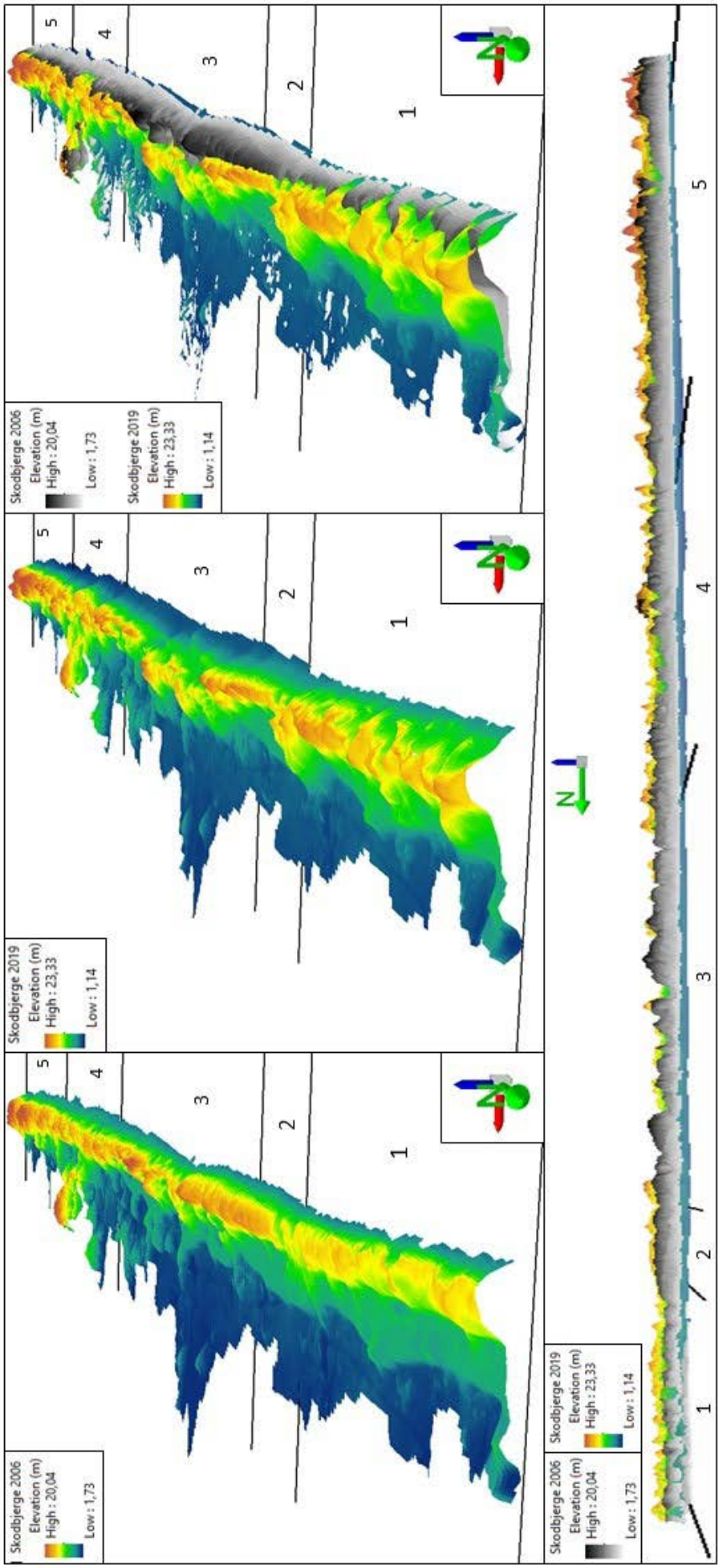

Figure 6-4: The DTMs from 2006 and 2019 have been clipped to the extent of the study area (seaward and landward boxes) and their height is increased in ArcScene with a factor 4. The three maps show the TM 2006, the TM 2019, and one where both models are shown to illustrate the change. The rectangular box at the bottom is included to illustrate changes in height seen from the sea side. The 2019 DTM is 30 % transparent at the bottom so the heights of dunes below are visible.

6.2 Volume analysis

The overall volume changes in the seaward box and the landward box are comparable over time (Figure 6-5). There seems to be a pattern for periods where erosion in the seaward box results in accumulation in the landward box e.g. period 1 (2006-2008). Although the volumes are different as regards erosion and accumulation, the magnitudes seem to be comparable. This also shows a close to balanced sedimentary budget for the total stretch, at least within the planimetrically defined boundary used for this study and despite the dune face retreat. This result was found to be particularly interesting as previous studies disregarded the sediment transport across the dune top to the leeward area as it has been considered insignificant. Most of the stretch has experienced dune face retreat during the study period and several blowout sections have developed forcing aeolian deposition into concentrated areas of accumulation. The balance between erosion in the seaward box and the accumulation in the landward box does not tell us whether the dune is simply migrating landward or primarily increasing in height, but it does reflect a sedimentary budget in balance between erosion at the dune face and accumulation landward of the dune crest.

Despite comparability in sediment exchange between seaward and landward boxes, the results are varying along the study area, both spatially and temporal. Figure 6-6 and Figure 6-7 show volume changes for landward and seaward boxes respectively. Furthermore, Appendix B shows the volume change of the seaward and the landward boxes for each section during the study period.

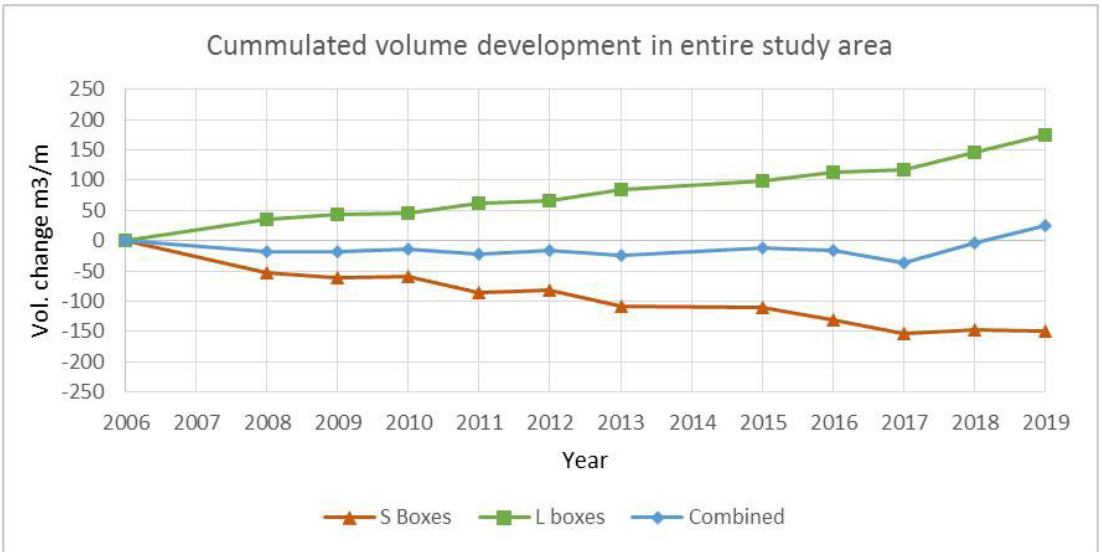

Figure 6-5. Cummulated volume change (m³/m) of the study area relative to 2006. Green is the total volume change in seaward boxes, red is the total volume change in landward boxes and blue is the total for both landward and seaward boxes.

6.2.1 Section 1

The northernmost section shows by far the lowest erosion rate (S1) compared to remaining seaward boxes, but still box L1 is one of the boxes increasing the most in volume over time. The seaward box is exposed to a constant but small erosion through the study period. This results in a total volume deficit of approx. 32 m³/m, whereas the landward box is exposed to a much larger total accumulation of sediment through the study period of approx. 200 m³/m. Volume addition in L1 increases slightly during the study period, but the period between 2017 and 2019 shows a near exponential increase in volume. This could likely reflect the boundaries used for the boxes. As the boundary between seaward and landward boxes is defined at the erosion front between 2006 and 2019, periods from 1 to 9 might have deposited some of the aeolian sediment in the seaward boxes just inland of the previous dune face, which is no longer the case as the dune crest has reached the boundary. Furthermore, an increase in erosion can be expected if the beach moves parallel with the dune face. However, this is not the case, and in periods 10 and 11, S1 volume only decreases slightly. This consideration is valid in all sections.

6.2.2 Section 2

Until 2011 S2 shows the same stability in the erosion rate as S1, but in the period between 2011 and 2013 an abrupt period of massive erosion occur and acute erosion from the sea erodes the dune face. From 2013-2014 the volume of the seaward box increases and this period is followed by small fluctuations in the volume change, but from 2016 to 2019 the volume increases. This results in a total erosion of approx. 136 m^3/m of the seaward box through the study period. L2 is the landward box which receives the lowest volume of sediment for all periods, and it even shows decreasing volume for periods 3, 5 and 9. From 2017-2019 the accumulation rate increases. This results in accumulation of approx. 74 m^3/m through the study period.

6.2.3 Section 3

The sediment deficit in S3 compares well with the accumulation in L3. However, the volume decrease in S3 is slightly higher than the accumulation in L3 between 2006 and 2017. There is an indication of acute erosion taking place in the dune face between 2012 and 2013, similar to the one seen in section 2. In the period between 2017 and 2019, the volume increases in L3 while the volume in S3 remains close to stable. The stability in S3 between 2017 and 2019 is comparable to the situation between 2013 and 2015, but the difference for the period between 2017 and 2019 is that the volume addition in L3 is not correlated to any deficit in S3. This indicates that a general addition of sediment is taking place, and this must come from outside the study area. This volume increase between 2017 and 2019 is found in all landward boxes without exception. The magnitude differs between the boxes but all show the same tendency in volume increase.

The total change of S3 through the study period is a deficit of 227 m^3/m and the total volume addition to L3 through the study period is 212 m^3/m.

6.2.4 Section 4

S4 shows a volume development comparable to that in S3, but not of the same magnitude. Despite the differentiated morphology of the dune face, accumulation in L4 is comparable to the accumulation in L3 also in magnitude and volume increase. There is almost no change in the volume of S4 between 2017 and 2019. Section 4 is exposed to an overall accumulation of sediment between 2006 and 2019 but this is mainly a result of the significant volume increase in L4 from 2017 to 2019. The total volume deficit of the seaward box through the study period is 177 m^3/m. The landward box is exposed to an additional volume of 202 m^3/m through the study period.

6.2.5 Section 5

Section 5 is one of the most stable sections when referring to the exchange of sediment between seaward and landward boxes. The overall volume development of the seaward box is relatively constant with a total volume deficit through the study period of 114 m^3/m. During the study period the volume of the landward box has increased with 127 m^3/m.

As presented for all other sections, there is stability in the volume of the seaward box between 2017 and 2019 and there is an increase in the volume of the landward box. This results in an overall volume increase for the study period. The combined effect of stability in the seaward boxes, and increase in the landward boxes shifts the overall trend from decreasing volume to increasing volume.

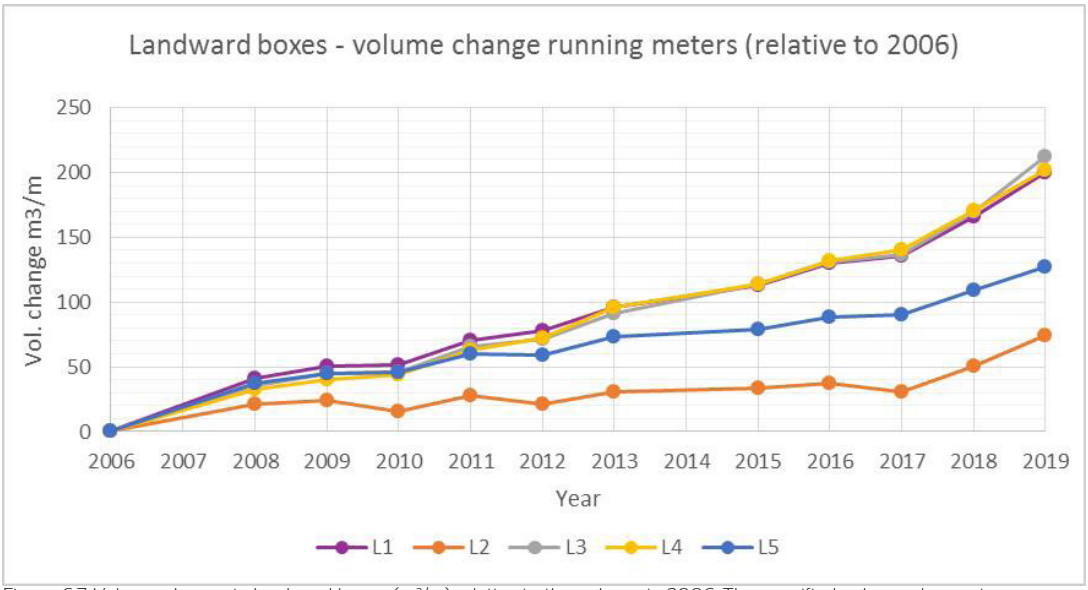

Figure 6-7. Volume change in landward boxes (m³/m) relative to the volume in 2006. The specified volume change is per running meter. Note that the individual stretches are different in length and can therefore not be directly be compared to the accumulated model. This underlines the variability along the study area.

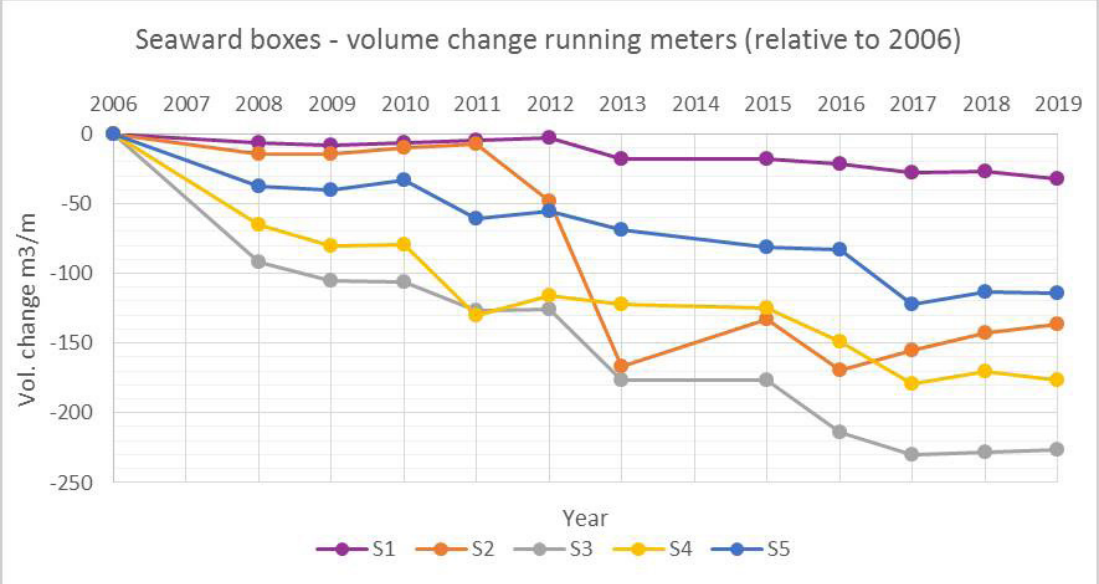

Figure 6-6: Volume change in seaward boxes (m³/m) relative to the volume in 2006. The specified volume change is per running meter. Note that the individual stretches are different in length and thus cannot be directly compared to the accumulated model. This underlines the variability along the study area.

6.3 Changes in the safety level

Analysis of changes in the safety level in relation to natural dune development is the focus of this chapter. The analysis is based on figures showing the planimetrical area at the 4.5 m contour (Figure 6-9), changes in volume above the 4.5 m contour (Figure 6-8), changes in the planimetrical position of the 4.5 m contour between 2006 and 2019, difference map (Figure 6-10) and a graph showing the fluctuation in dune width at 4.5m for all LIDARs (Figure 6-11).

To maintain the safety level at Skodbjerge the dune needs to be at least 40 m wide at 4.5 m height. The current safety level is acceptable, as the dunes along the study area qualify for the criteria (Figure 6-11). For most of the stretch, the general tendency is that the dunes are receding due to increasing longshore gradient in transport capacity, but the 4.5 m contour shows fluctuation over time with natural variations. This is due to ramp build up, acute erosion, accumulation at the dune leeside etc. Volume in the landward boxes is generally increasing, and the primary volume increase is mostly taking place in the blowout

sections of the dunes. The prior volume analysis does not reflect the changes in the safety level, which is why the changes in the 4.5 m contour between 2006 and 2019 (Figure 6-10 and Figure 6-11) are included. Despite a retreat in the 4.5 m contour, there might be an increase in the volume above 4.5 m. Therefore, an analysis focusing on the volumetric changes above the 4.5 m contour (Figure 6-9) and average width of the 4.5 m contour (Figure 6-8) in each section is included.

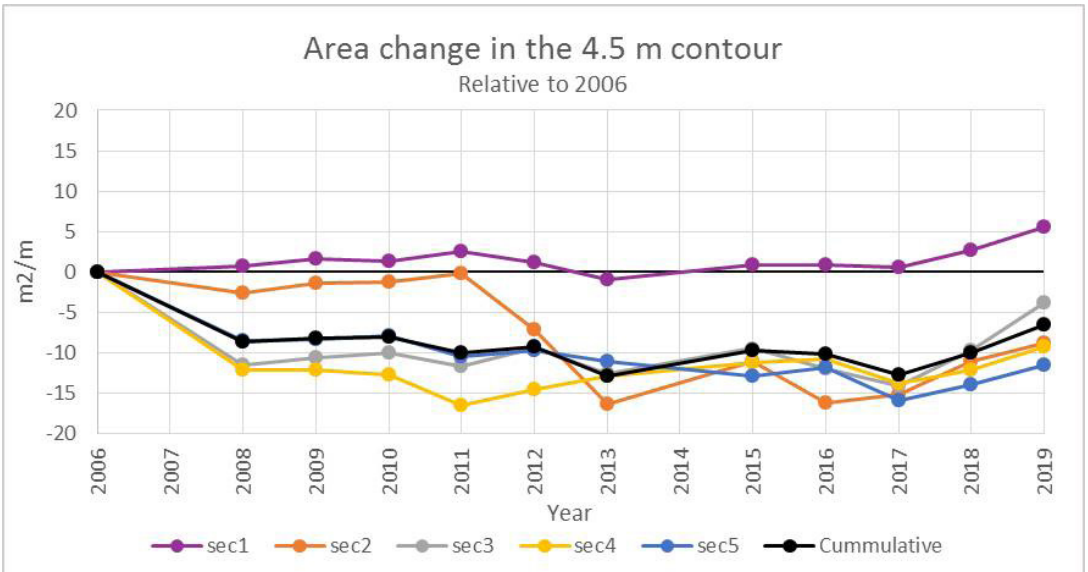

Figure 6-9: The area above 4.5 m is divided by the longshore length of the section. It can therefore be seen as changes in average width.

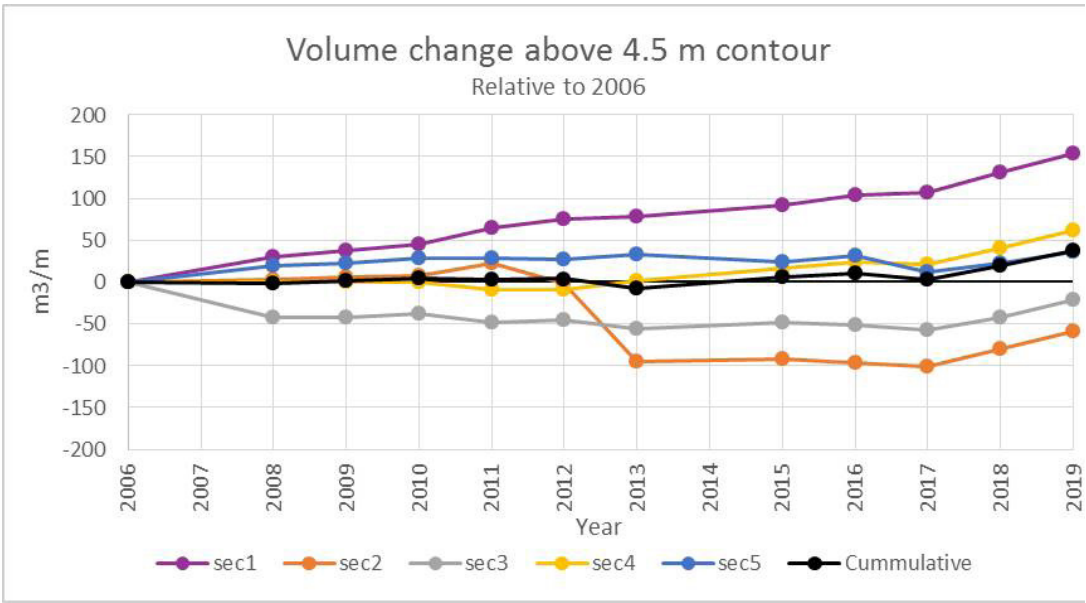

Figure 6-8: The volume above 4.5 m divided by the longshore length of the section. The result is volume change per running meter.

6.3.1 Section 1

Section 1 is the northernmost box of the study area. The volume of the dune above the 4.5 m contour increases for the whole study period, and only a slight decrease in area is seen between 2011 and 2013. Following 2013, the area above at the 4.5 m contour increases until 2019 where the most pronounced increase takes place between 2017 and 2019. The increase between 2017 and 2019 is also evident in the volume development, as the volume increase in this period is higher than in the previous years. Generally, the average elevation above the 4.5 m contour has increased with 1.3 m.

The 4.5 m contour in the dune face is only retreating in the southernmost part of section 1. The 4.5 m contour of 2019 in the middle and northern part of the section fluctuates around the 2006 position despite smaller fluctuation during the various periods. For most of the stretch the 4.5 m contour on the leeside of the dune is migrating landward which corresponds with the slight increase in dune width at the 4.5 m contour. The elevation changes and primary accumulation are found in the depositional lobes of the blowout sections but are also evident in most of the dune between the blowouts. The seaward box (S1) shows hotspot erosions in the deflation basins of blowouts.

6.3.2 Section 2

Section 2 presents the shortest stretch of all sections but it also reveals the largest decrease in volume. This was caused by acute dune erosion between 2011 and 2013. Despite a large decrease in both volume and area of the 4.5 m contour between 2011 and 2013, both volume and area seem to generally increase between 2013 and 2019. Again, 2017 to 2019 shows a remarkable increase in both area and volume.

An increase of volume in section 2 takes place just landward of the dune crest, as seen from L2 in Figure 6-10. The volume increase is more evenly distributed in L2 than in L1, and only a small area in the southern part of L2 indicates a slight hotspot accumulation. This section generally shows a more stable dune face and the dune crest is generally homogeneous in height. The 4.5 m contour in the dune face have migrated 10 m landward on average while only slight landward movement of the leeside 4.5 m contour is found. The result is a net decrease in dune width, mainly caused by the acute erosion of the dune face between 2011 and 2013. Looking to Figure 6-11 the dunes have generally widened in section 2 between 2016 and 2019. This can be attributed to a seaward migration of the 4.5 m contour in the dune face.

6.3.3 Section 3

Section 3 shows a decrease in volume above 4.5 m between 2006 and 2008, which follows the same trend as sections 4 and 5. The area at the 4.5 m contour also decreases during this period, but this is not the case for sections 4 and 5. Most decreases in this area can be attributed to acute erosion in the dune face between 2011 and 2013, which also affected sections 1 and 2. Despite changes in dune width between 2006 and 2017, the dune width fluctuates around the same values in time. The volume above 4.5 m does not show significant increase nor decrease in that period. Between 2017 and 2019 there is an increase in both area and volume. The increase of the area is slightly higher than the volume increase, and the average height therefore decreases.

The 4.5 m contour in the dune face has retreated landward, but due to the landward movement of the 4.5 m contour on the leeside of the dune, the reduction in average width is only 3.5 m on average for the entire section. For some parts of the section, the development is close to an inland parallel displacement of the dune and the dune width is found to both decrease and increase locally, as seen in Figure 6 11. This section is also the one in which the aeolian depositions reach furthest inland. This is both evident from difference maps but also from visual inspection of available orthophotos. The dune in section 3 is relatively stable with regard to average height but this section shows the largest effects of depression and blowouts in the dune. From drone imagery, it was determined that the dune face for a large part of this section consists primarily of a stone paved ridge facing the sea, while dune tops have either eroded or retreated inland due to development of blowouts.

6.3.4 Section 4

Between 2006 and 2011 the area at the 4.5 m contour in section 4 shows the largest decrease of all boxes. In the following periods from 2011 to 2019 and especially between 2017 and 2019, the area at the 4.5 m contour increases with nearly 1 m²/m/yr. The volume above 4.5 m only gets below the 2006 level between 2010 and 2012, but for the remaining periods, the volume increases despite a reduction in average width. The overall tendency is again highly affected by the period between 2017 and 2019 in which the volume increases more than at any time before in the study period.

The 4.5 m contour in the dune face has, in general, retreated evenly on the stretch. The 4.5 m contour on the lee side of the dune has migrated landward in the northern end where depositional lobes from

blowouts have migrated landward. Additionally, filling of bowls underneath 4.5 m is registered, also as a result of accumulation in depositional lobes of blowouts. Hotspot accumulation primarily dominates in the depositional lobes of blowouts. Section 4 also shows sporadic increase and decrease in dune width over time, and the section also shows the widest dune at 4.5 m which is explained by the inland dune ridge welding together with the foredune in the middle of the section (Figure 6-11).

6.3.5 Section 5

Section 5 shows the largest decrease in area at the 4.5 m contour of all sections. The decrease in area is a result of the landward movement of the 4.5 m contour in the dune face. The retreat decreases from north to south. The lee side 4.5 m contour is close to constant between 2006 and 2019. The dune width increases between 2017 and 2019, as a result of seaward migration of the dune face 4.5 m contour in periods 10 and 11.

The volume above the 4.5 m contour proves to be relatively stable between 2008 and 2016. A slight decrease between 2016 and 2017 is followed by a volume increase between 2017 and 2019, which is comparable to that in remaining boxes, but smaller. This gives a slight decrease in average height. The primary increase in volume is again found in the depositional lobes of the blowout sections. Hotspot erosion is also identified in a small inland blowout in the southern end of L5.

6.3.6 Summary

Retreat of the seaward 4.5 m contour does not necessarily equal a negative sedimentry budget of the dunes. A retreat in the dune face 4.5 m contour does not directly correlate with a decrease of the dune volume, as accumulation may take place in the dune top as well as inland. Neither does a retreating dune face directly reflect a decrease in dune width as it was found that landward migration of the leeside 4.5 m contour takes place on several parts of the stretch. The evolution of dune width and volume must therefore be assessed in both a holistic and temporal perspective to truly grasp the changes in the safety levels. Only section 1 shows an increase in both area and volume above 4.5 m. Despite the retreat of the 4.5 m contour, the volume above the 4.5 m contours increases for sections 4 and 5. Sections 2 and 3 are both showing a decrease in area and volume between 2006 and 2019, but for all other section the periods 10 and 11 (2017-2019) generally show increase in area and volume.

The safety level must be considered decreasing if considering the dune width at the 4.5 m contour, only. However, the dune volume actually increases despite narrowing which results in an increase of average dune height. Furthermore, the dune face 4.5 m contour have been found to migrate seaward following significant retreats. Area, width or volume increase is therefore local. The primary volume increase is found in the depositional lobes of blowouts, which have assisted in landward migration of the lee side 4.5 m contour. The period between 2017 and 2019 again shows an impressive increase in volume and area above the 4.5 m contour. It is not possible to determine the reason for this volume increase from the analysis carried out, but it provides a foundation for further analyses in future projects.

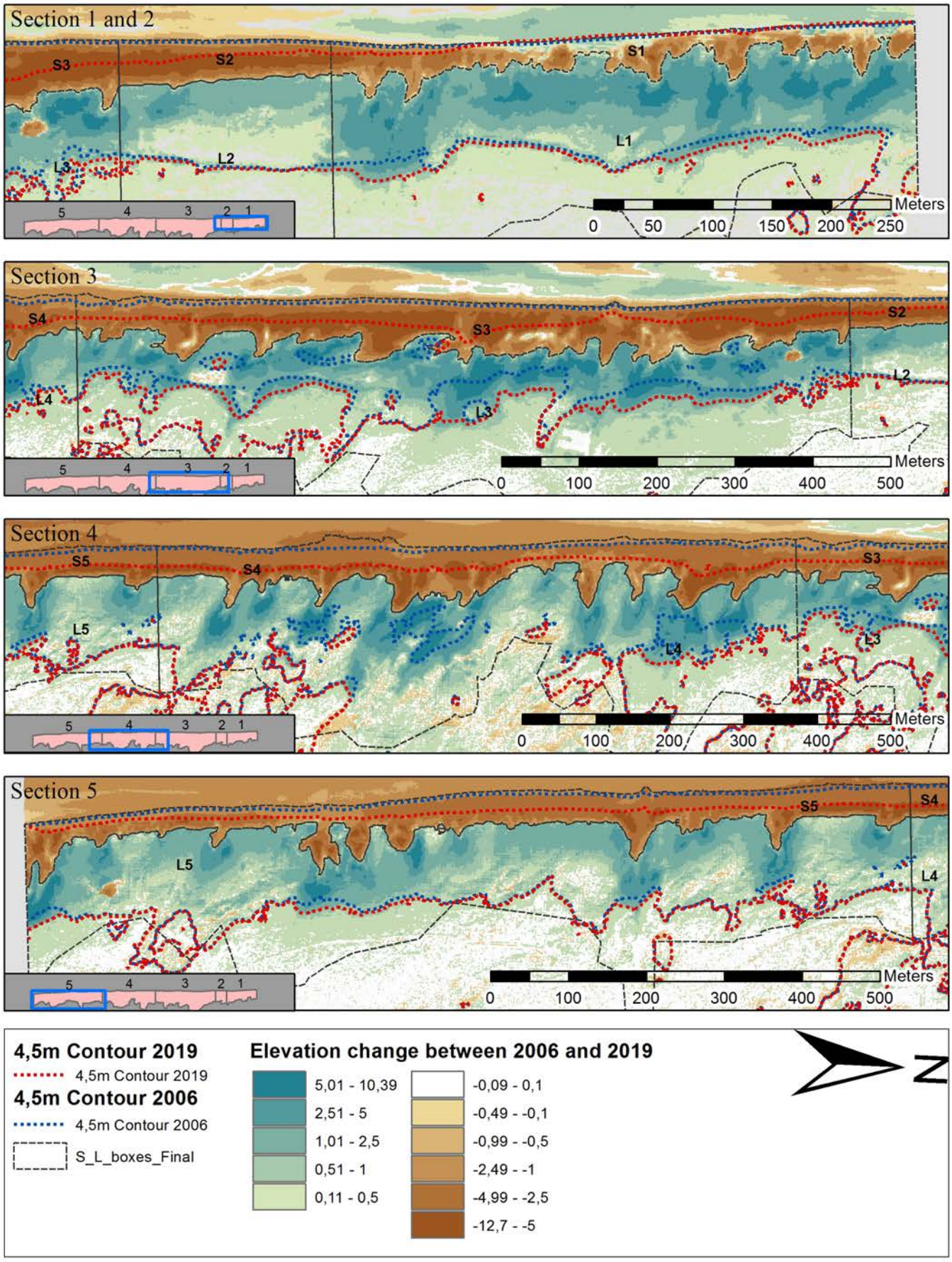

Figure 6-10. The base map is a difference map of elevation change from 2006 to 2019. The blue dotted line is the 4.5 m contour in 2006 and the red dotted line is the 4.5 m contour in 2019. The black dotted lines are the boundaries of the sections and the seaward and landward boxes.

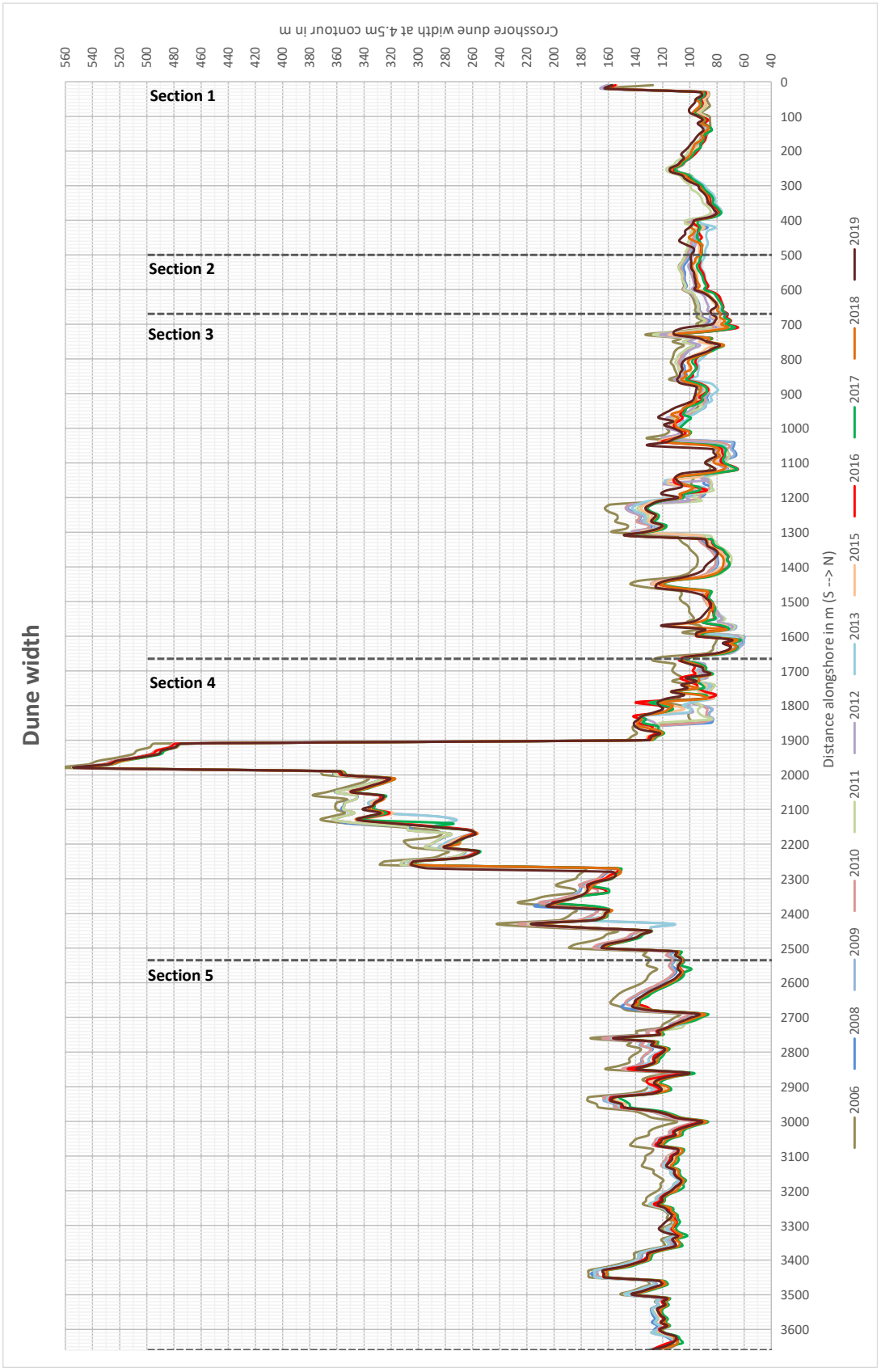

Figure 6-11: The dune width at the 4.5 m contour is shown for all available LIDAR-scans. Sectional divisions are inserted at the same place as they appear in other figures and maps throughout the report. Dune width is calculated for every 10 meters along the study area and the method for extraction of the width is described in chapter 4.

6.4 Correlation between wind and sediment transport

To analyse the relation between wind and sediment transport, a relation test between the number of hours above the threshold fluid velocity and the volume of eroded and accumulated sediment is performed. Table 6-1 presents a summary of each period for wind directions between 170° and 360° and wind speeds above 8.9 m/s. The number of hours with wind speeds above 8.9 m/s is presented for each period, as well as the percentage of the total period in which wind speeds between 170° and 360° have been above 8.9 m/s. Furthermore, average wind speed and average wind direction are included for description purposes. The table only presents winds between 170° and 360° and resampling into closed hourly bins is performed after winds with direction between 0° and 169° have been filtered out.

In Table 6-2, the total accumulation and erosion in each period are presented. These volumes represent the total changes along- and across the entire study area. These are found by utilizing the clip and surface volume method. Although errors might occur, they are minimized as the full area is now analysed rather than singular boxes, NoData grid-cells where set to 0 m elevation change.

The table is based on wind data between 170° and 360°					
Period	Hours in period (total)	Hours in period above 8.9 m/s	Period above 8.9 m/s of total (%)	Average wind speed (Direction 170-360)	Average wind direction (Direction 170-360)
1	18648	6520	35.0	7.8	261
2	7608	2019	26.5	7.6	259
3	12552	3500	27.9	7.4	265
4	11184	3626	32.4	8.2	253
5	7968	3192	40.1	8.1	261
6	9456	2366	25.0	7.5	260
7	11808	4040	34.2	8.1	253
8	8568	2414	28.2	7.8	256
9	8928	2499	28.0	7.4	260
10	8544	2523	29.5	7.6	261
11	11040	3385	30.7	7.7	266

Table 6-1. Summary of each period for wind directions between 170° and 360°. The total number of hours during the period, number of hours with wind speed above 8.9 m/s, percentage of the total period in which wind speeds have been above 8.9 m/s, average wind speed and average wind direction.

Change between LiDAR scans (10^3 m^3)			
LiDAR	Period	Accumulation	Erosion
2006 and 2008	1	152	-215
2008 and 2009	2	51	-52
2009 and 2010	3	73	-58
2010 and 2011	4	102	-137
2011 and 2012	5	92	-66
2012 and 2013	6	78	-112
2013 and 2015	7	103	-58
2012 and 2016	8	72	-89
2016 and 2017	9	53	-123
2017 and 2018	10	158	-36
2018 and 2019	11	158	-55

Table 6-2. Volume change between LiDAR scans calculated as accumulation and erosion in each period.

Figure 6-12 presents the results when plotting the number of hours above the threshold (8.9 m/s) with the amount of eroded or accumulated sediment. It is evident that there is no direct relation between the two. There are many elements, which are not included in this simple test, and the results underline the fact that the factors influencing sediment transport are not limited to just the wind.

A test was also conducted for thresholds of 4 m/s, 6 m/s, 8 m/s, 10 m/s, 12 m/s, 15 m/s and 20 m/s, and none of the tests showed a good fit as seen from Table 6-3. All tests are shown in diagrams in Appendix C. Best fit was found for erosion and 20 m/s with R2 at 0.55, but still with significant outliers. Regarding accumulation, the best fit was found for wind speeds at 10 m/s, 12 m/s and 15 m/s with R2 ranging between 0.35 and 0.4. Still there is not at direct correlation between wind regime and erosion, nor accumulation. Figure 6-12 presents two main issues in the test. Period 1 (6520 hours) affects the fit as it steers the regression analysis by skewing the fit, furthermore accumulation in periods 10 and 11 are significantly higher than in the remaining periods.

However, there are some relatively good results if we consider the numbers grouping around the regression line in accumulation tests in appendix C. If we remove the two significant outliers the R2 values increase to >0.9 for accumulation. The two significant outliers are periods 10 and 11, which are extraordinary as regards accumulation. The relative relation between accumulation and wind was unexpected but is likely to be explained by the analysis extent within the planimetrically defined boxes. Measured erosion is restricted to box limits, while accumulation is not. The aeolian sediment transported into the box can be transported from both across and along the coast, therefore the accumulation analysis is not restricted to a distinct area, as is the case with erosion. The state of the beach can be highly varying in both time and space as regards for instance height, volume, and sediment availability, but when analyses are carried out for large areas and long time periods the changes are likely to be more stable over time. Furthermore, the erosion parameter in this test is affected by acute erosion on several occasions, which is not the case for the accumulation parameter, at least not to the same extend.

Wind speed m/s	Accumulation (slope)	R2	Erosion (slope)	R2
4	10.3	0.29	-17.1	0.48
6	13.1	0.28	-21.6	0.46
8	20.0	0.30	-31.4	0.44
8.9	25,5	0,33	-38,2	0,43
10	35.1	0.35	-50.1	0.42
12	72.1	0.40	-102.7	0.48
15	208.5	0.38	-285.6	0.42
20	841.8	0.06	-3192.0	0.55

Table 6-3: Several tests between measured transport and different wind speeds have been conducted. The linear fit is described in this table. All models can be found in appendix C.

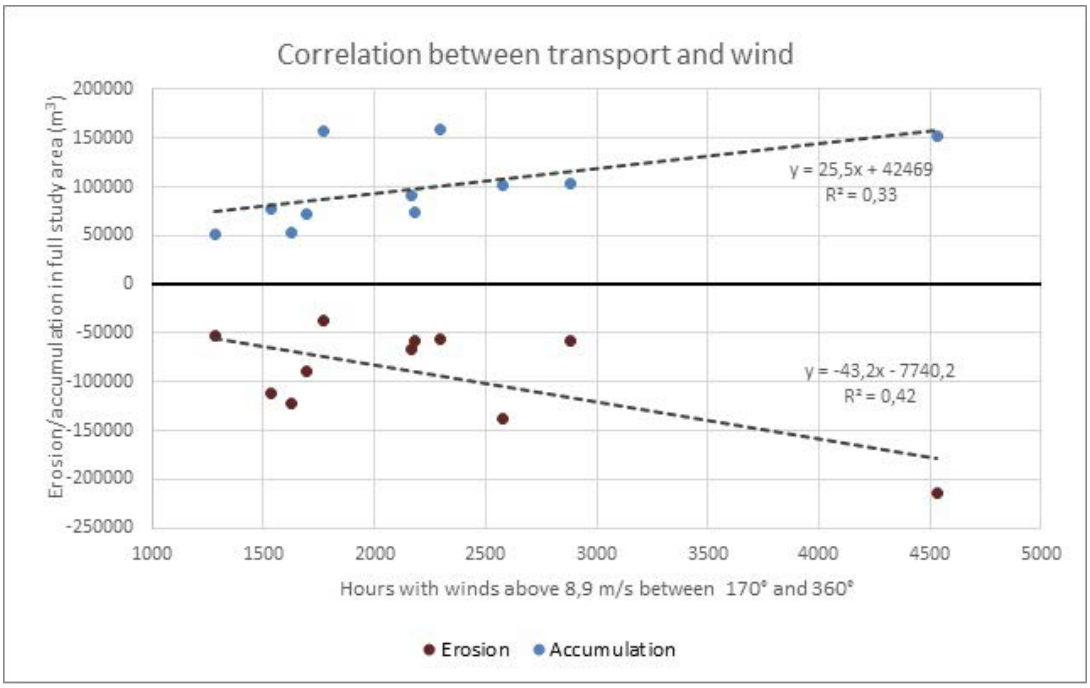

Figure 6-12: Test of the fit between erosion/accumulation and number of hours with winds above the critical threshold fluid velocity 8.9 m/s (z=25 m). Description of results is found in the text.

7. Discussion

In the following section, a discussion of the data, methods and results will be presented. For the discussion of the data and methods, subjects found to be most relevant for the study will be discussed, while the discussion of the results is based on the hypotheses and research questions.

7.1 Data and methods

7.1.1 LiDAR data

When performing qualitative and quantitative analyses on the LiDAR scans, one must keep in mind that several elements can disturb the quality of the datasets. The time of year for conducting the LiDAR scans and vegetation intensity might influence the production of a DTM as low vegetation intensity allow more points to hit the surface compared to situations with high vegetation intensity. Slight distortion of the point measurements might also influence the overall mapping, but one must especially consider the difference in grid sizes when quantification analysis is performed for the datasets.

One way to handle these inconsistencies is correction of raster datasets from the original LAZ data files. The raw LAZ files are available but correction were not made, as the process would be too time consuming for this given project, and there is no guarantee for increasing the accuracy of the data sets. Despite obvious concerns between the different LiDAR raster datasets, no correction to the data sets has been performed as the potential outcome might disturb the models even more.

7.1.2 Division of stretches

For volume analyses of a very dynamic dune area on a decadal time scale it can be difficult to define fixed boundaries that are appropriate for the entire study period. Between 2006 and 2019 the dune face retreats and there are large spatial and temporal variations in the development of the dune area. It was decided to use planimetric fixed boundaries as one of the focus areas was to describe the sediment budget, and therefore the planimetric fixed boundaries ensured that the area analysed stayed the same over time. However, when defining the fixed boundaries used for this study it was an aim that the boundaries would represent that part of the dune area which was mostly affected by aeolian processes but it should also reflect the area of the safety level. Based on the return periods for water levels in the area, as well as considerations related to the safety level, the seaward boundary of the seaward box was defined by the 4 m contour from 2006. Although the boundary was set so that primary changes seen in the boxes are forced by aeolian sediment transport, this was not completely satisfactory as the dune face was exposed to undercutting and acute erosion during the study period. Furthermore, the 4 m contour retreated significantly between 2006 and 2019, and it is very likely that volumetric changes in some of the seaward boxes are a result of both marine and aeolian processes.

The boundary between the seaward and the landward box is based on the boundary between erosion and accumulation in the dunes from 2006 to 2019. This distinct line between the area of erosion and the area of accumulation is found to correspond to the location of the dune crest of 2019. This way of dividing the area means that the retreating dune face is located more seawards in the beginning of the study period and the area of accumulation leeward of the dune crest is located in the seaward box. During the study period the dune crest and the leeward area of accumulation moves landward until 2019 where it is represented by the boundary between the two boxes. This change in location of the dune crest is also reflected in the annual elevation changes in the difference maps. The dune crest retreats during the study period, and in the beginning of the period it is d located in the seaward box. The seaward box can therefore be subdivided into an outer part of erosion and an inner part of accumulation.

The inland boundary was determined from NDVI analysis, which was setup in order to find the extent to which the aeolian sediment affected the vegetation. This resulted in a detailed inland line, which despite good results, needed manual correction to the extent of depositional sheets detected in available orthophotos from the whole study period.

It would have been an obvious thought to define the inland boundary to the precise line where no elevation changes were observed, but this proved to be much more difficult than first assumed. Several difference maps showed inland changes far beyond the extent of the area affected by aeolian processes. These changes where considered as scatter and the reason why they appear can be attributed to the differences and inconsistencies between LiDAR datasets. The terrain changes were especially found to take place in the older dune ridges inland of the foredunes, and changes were both shown as increases and decreases in height between different years. However, it is possible that some sediment has been deposited as far inland as in these older dune ridges. The terrain changes are expected to be the results of settlements in the dune layers, inaccuracies in the LiDAR rasters, difference between DTM point recognition and change in vegetation density over the years or different point density pr. m².

Despite these inaccuracies and limitations in the use of fixed boundaries it is found that the boxes defined for this study are suitable for the purpose.

7.1.3 Variations in spatial resolution of DTMs

Volume calculations in this project are based on three different analyses using two different methods – "Clip and surface volume" and "Zonal statistics as table". As discussed above, concerns regarding the differences between LiDARs were considered.

Volume calculations internally in defined boxes:

One initial concern was the difference in cell sizes in different raster models and how this would affect the volume calculations. The two approaches for volume calculations were therefore tested. The output file from both methods ("clip and surface volume" and "zonal statistics") contain an area on which the volume is calculated. Table 7-1 presents the total planimetric area of the landward and seaward boxes. The combined areas of all seaward and landward boxes (from both methods), and the difference between polygon area and analysis area are presented in three columns, one for each cell size of the rasters. There are differences between polygon areas and analysed areas for both approaches. Differences are far larger in the "clip and surface volume" method than in the "Zonal statistics" method. The reason is not straightforward and was therefore analysed in more detail.

Total area in polygon 762272.5 m²	Clip and surface volume method (m²)	Difference between analysed area and polygon area (m²)	Zonal statistics method (m²)	Difference between analysed area and polygon area (m²)
Total area included (1.6 m grid)	739384.3	22888.2	762127.4	145.1
Total area included (0.5 m grid)	755090.5	7182.0	762230.3	42.3
Total area included (1.0 m grid)	748044.0	14228.5	762194.0	78.5

Table 7-1: The area output from the volume analysis is presented and referenced to the total area of the polygon feature of the landward and seaward boxes – the total polygon area is presented in upper left corner.

Clip and surface volume approach:

When the raster layer is clipped to the polygon extent, it includes internal cells and cells closest to the feature boundary, so cells are not necessarily included just because they are in contact with the line. Larger areas along the feature boundaries will therefore not be represented. Using the input feature for clipping geometry ensures that the polygon feature is used to clip the raster and thereby cells along boundaries between boxes is only represented in one of the boxes.

Along the feature boundary where no adjacent box exists, there will be larger exclusion of cells, which explains the difference in extent between clipped and actual box areas. The total area varies with more than 15.000 m² from 1.6 m grid to 0.5 m grid, but this difference decreases significantly due to cell size, as

smaller cells mean that more cells are found along the boundaries and blanks that were not covered by the larger cells are now filled in. As the errors regarding area and analysis extent of the "Clip and surface volume" method was far more pronounced than those found in the "zonal statistics" tool, the former method was only used to identify total erosion/accumulation in the difference map and for the volume/area analysis above the 4.5 m contour. The ability of the tool to set a "reference plane" was utilized in the difference maps to analysis changes above and below 0 m, to obtain the total eroded and accumulated volumes.

"Zonal statistics as table" approach:

The automated resampling in the "zonal statistics" tool proves much more precise when handling the polygon boundaries. This is evident when we look at Table 7-1 as the difference is significantly lower than that seen for the clipping method. However, a main concern is that the tool does not give an actual raster output, and it is therefore uncertain whether the tool includes the same cells in more than one box. To test the output the "zonal statistics" tool was performed, as it gives an actual raster layer. It was found that resampling is performed automatically within each feature, on the basis of the input raster grid cell size. The output raster grid is "best fit" within the polygon boundaries with the input cell sizes. The resampling is made on the basis of the nearest cell. The data is thereby manipulated, which originally should be avoided.

In order to avoid manipulation of the data, a more correct practice is to use a raster layer instead of polygon boundaries for defining the area extent. This is done by creating a "zone layer", on the basis of the polygon boundaries with raster resolution equal to the "value layer" (here LiDAR datasets) see Figure 7-1. In ArcMap this can be done by converting the defined box polygon to a raster layer with the "feature to raster" conversion tool. The value field must be set to the string field with the boxes' name information (S1, S2, S3 etc.) so all cells in the zones have the string value matching their box name. To ensure that the new boundary raster grid fits correctly onto the value raster grid, environmental settings in the conversion tool must be set with the "snap raster" being the value raster we wish to examine (here the value raster which are the LiDAR datasets). This is set under processing extent in the environmental settings of the "feature to raster" conversion tool. Naturally, the "zone layer" must be made for all three grid-sizes. These zonal layers can be applied in both methods for either clipping extent or for input zone layer in the "zonal statistics as table". The output in the zonal statistics as table tool is as seen in Figure 7-1. A simpler method is to set the processing extent with snap raster to the "value raster" in the "zonal statistics to table" or "clip" environment. Setting the snap raster in zonal statistics means that resampling is not performed, and that the actual grid of the input is used. This results in the same output extent as in the clipping method.

When choosing not to resample the data set at the beginning, this is mainly to avoid manipulation of the existing data sets. Despite the efforts, some resampling has been conducted in the analysis steps and therefore there may be some slight offsets in the volumes and difference mappings. The results of the volume analyses did, however, show the same tendencies and the results are accepted for this analysis. However, there is a need to further consider the "most correct" method, or at least compare different studies which included LIDAR datasets, as the output results cannot be compared unless these considerations are made.

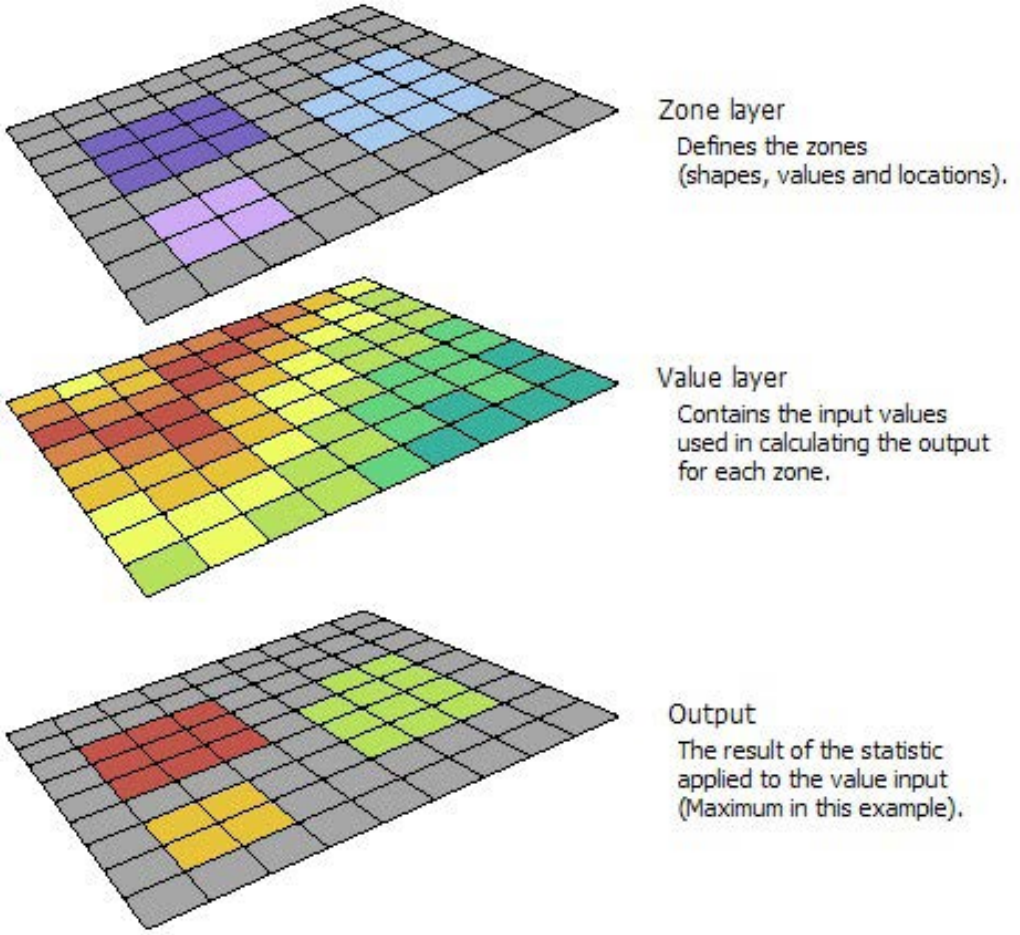

Figure 7-1: The figure presents the concept of using zone layers in the same grid format as the value layers. The zones are defined by the value or string in the individual cell. Figure is reproduced from (ESRI, 2019).

7.1.4 Wind measurements

The wind measurements are conducted more than 10 km away from the study area and throughout the report it is assumed that the wind measurements are representative for the local wind regime in the study area. In reality wind direction and speed can change along the coast, and the local wind pattern is likely to vary significantly across and along the beach and dunes. Furthermore, the wind measurements are conducted more than 500 m inland in the middle of the harbour town of Hvide Sande. Despite measurements being conducted at the height of 25 m, it is not unlikely that wind measurements are affected by turbulence due to the presence of various obstacles, such as windmills etc. The assumption of comparable wind regimes between the site of measurement and study area remains the most reasonable assumption, as there are no local wind measurements with which to compare the Hvide Sande measurements. The wind measurements from Blaavand could have been used as these measurements are conducted close to the coast. However, the distance to Blaavand is 40 km, which is four times the distance to Hvide Sande, and despite obvious disadvantages at the Hvide Sande station, the distance was considered the main factor in relation to the comparability of wind regimes.

It is difficult to establish whether the low correlation values between wind and accumulation/erosion is caused by gaps in wind data, the difference in wind regime between study area and measurement site, or other factors. Again, as there is no foundation for comparison at the study area it is likely the best correlation we are able to procure. The gaps in the data sets could have been filled with modelled data, if a correlation between true and modelled data was performed, but this was outside the scope of this study. The test between transported mass and hours of wind above the critical threshold fluid velocity showed low correlation with both erosion and accumulation. However, there were indications of some relation between the accumulated mass when outliers were filtered out. It would seem obvious that there

is a correlation between wind and transported mass as the sediment transport is dependent on the wind. However, as established in other studies, there are several elements in beach morphology and processes, which restrict the potential transport capacity and these elements are not included in this study.

7.2 Results

In this report, the spatial and temporal variation in dune morphology has been examined from a variety of analyses. In the following chapter, we revert to the hypothesis and research questions which were presented in chapter 1. The hypotheses will be presented individually with an evaluation of the results contributing to answering the research questions.

Accumulation of sand in the dune area is primarily found on the lee side of the dune crest and in the depositional lobe of blowouts. Erosion is primarily found at the dune face and in the deflation basin of blowouts.

- Which areas of the dune are dominated by erosion and accumulation, respectively?

Based on difference map of the elevation change from 2006 to 2019 it can be established that accumulation is dominating the landward boxes. Hotspot accumulations are found in the depositional lobes of blowouts, but sheets of accumulated sediment also occurs inland of the dune crest. Depositional lobes as single morphological features are mostly pronounced in sections 4 and 5, whereas the depositional lobes in sections 1, 2 and 3 have merged and are less well defined. In the southernmost part of section 5 a small area of erosion is found in the landward box. This is a deflation basin detached from the dune face.

Erosion dominates the seaward boxes and deflation basins of blowouts. The number, shape and size of blowouts vary along the study area. In section 1 the blowouts are relatively small but they are numerous, whereas almost no blowouts are present in section 2. In sections, 3 and 4 there are many blowouts and the blowouts are very large. Some of them even merge. In section 5 the blowouts are more separated but they are still relatively large. Despite the fact that the seaward boxes are dominated by erosion, accumulation at the dune face is measured along the entire stretch with temporal variations. There are tendencies of build-up in the dune face and some years even show accumulation in some of the seaward boxes.

The wind climate affects the amount of sediment eroded and accumulated in the dune area. The shape and orientation of the accumulated sediment reflect the dominating wind direction

- What are the effects of the wind climate on development of the dunes?

Based on difference maps it is established that there are alongshore variations in the shape and orientation of depositional lobes of blowouts. It is also found that the orientation of the deflation basins vary in alongshore direction. The difference map 2006-2019 indicates that the orientation of the depositional lobes is the same as the orientation of the deflation basin. This tendency is most visible in sections 4 and 5 where the blowouts are more separate and therefore it is easier to distinguish the different depositional lobes from each other. From this study, it is not possible to demonstrate that the dominating wind direction is reflected in the shape and orientation of the accumulated sediment.

Assessing the different LiDAR maps over time does not give precise indications of deposition corresponding to the predominant wind direction. Instead, changes indicate that dune face, blowout and beach topography create a far more complex relation between wind and deposition. It is assumed that the entire coastal stretch of the study area is exposed to the same regional wind field and the alongshore variations in orientation of the current deflation basin and depositional lobes are therefore a result of something else. It could be a result of local near surface flows caused by topographic steering rather than the regional wind field. Anthropogenic paths in the dune field are also likely to affect the development. In all sections it was found that blowouts cause the largest accumulations with hotspots in their depositional lobes. This indicates a topographical steering of the aeolian sediment across the dune via the blowouts.

To test the relation between aeolian transport and wind regime, the number of hours with onshore winds above the threshold fluid velocity were tested against eroded and accumulated sediment for each period.

No significant correlation between the two was found despite wind being the primary driver for aeolian sediment transport. The insignificant correlation between mass movement and wind regime is the result of a complex environment in which the transport capability can be limited by multiple factors. As there were no local wind measurements with which to compare the wind data, it is difficult to estimate the actual wind regime at the study site. The difference between the measured wind in Hvide Sande and the actual wind at the study site may also have affected the correlation. It was expected that the correlation would be low, as a variety of restraining factors are not incorporated in the methods used for this study and thus missing in the correlation. These factors highlight the fact that processes in relation to aeolian sediment transport and dune development are very complex and dynamic. This has been supported by many other studies, as well as in literature on the subject, as mentioned earlier (Christiansen et al.. 2004; Walker et al.. 2006; Bauer et al. 2009; de Vries et al.. 2012; Bauer et al.. 2012 etc.).

As there is a wide variety of possible parameters, it is difficult to pinpoint the most obvious factors affecting the sediment transport at Skodbjerge. Even so, the results from the volume calculations give good indications of areas and periods, which could be interesting to investigate further. For example, the periods 10 and 11 showed a significant increase in volume along and across all of the studied area. The scale and extent of the current study does not allow for a more in-depth analysis of the relation between the wind climate, restraining factors and the erosion or accumulation of sediment.

Aeolian transport of sediment and the presence of blowouts can cause considerable changes in the dune area, which in turn affects the safety level.

- Do volume and dune morphology change during the study period and is development on the lee side equivalent to that of the dune face?

Between 2006 and 2019 areas with the largest erosion and accumulation are not cross-shore related and the 4.5 m contours of 2006 and 2019 showed that the spatial changes of the dune width are highly different along the study area.

The volume analysis showed large differences between the amounts of sediment eroded in the seaward box and accumulated in the landward box in sections 1 and 2. However, in sections 3, 4, and 5 the volume deficit in the seaward boxes is balanced by the increase in volume in the landward boxes, and sections 4 and 5 are overall accumulating between 2006 and 2019.

Section 1 shows the largest accumulation in the landward box while the seaward box shows only a slight decrease in volume. The 4.5 m contour is almost unchanged from 2006 to 2019. Only the southern part showed landward migration of the dune face 4.5 m contour. For a small part of the section, the dune becomes slightly wider due to landward migration of leeside 4.5 m contour.

Section 2 is the section with the most stable and continuous dune crest. Only one small blowout is present. This is also the section with the smallest accumulation of sediment in the landward box. The retreat of the seaward 4.5 m contour and stability of the landward 4.5 m contour result in a narrowing of the width in the 4.5 m contour. The retreat caused by acute erosion decreased the safety level and scarped the dune face. This is likely to have resulted in a steepening of the dune face following 2011 to 2013, which can have reduced the potential accumulation in L2. The fact that no blowouts are present could also explain the low exchange of sediment from the beach area to the leeside of the dune crest compared to remaining sections.

Section 3 was different from all other sections, as the top section was found to migrate landward across the plateau of the dune reinforcement from 1994. Between 2006 and 2019 the overall volume for S3 and L3 decreases with 10 m³/m. This is mainly attributed to periods 9, 10 and 11 in which S3 shows stable volume while the volume in L3 has increased significantly. Despite several meters of retreat in the dune face 4.5 m contour, the average width in the 4.5 m contour of section 3 was only reduced with 3.5 m between 2006 and 2019. This is due to the aeolian fill of dune areas below the 4.5 m contour and landward migration of the leeside 4.5 m contour.

Section 4 was the only area where the dune face 4.5 m contour was affected by blowouts in relation to increased retreat near the upper parts of deflation basins (northern part of section 4). The 4.5 m contour on the dune leeside is almost unchanged in the study period, which results in a narrowing. Despite the narrowing of the dune the overall volume demonstrates an increase in section 4. However, this volume increase is dominated by a local increase in dune height in depositional lobes of blowouts. Some dune areas below the 4.5 m contour have been more or less filled through the study period as it was seen in section 3.

In section 5 the dune face 4.5 m contour retreated significantly in the studied period. The leeside 4.5 m contour did not migrate inland so no parallel displacement is found in this section. The dune therefore has become narrower. Despite volume decrease within S5 the volume increase in L5 balances the deficit with a slightly accreting volume between 2006 and 2019. This results in an overall increase in the height of the dunes and a slight landward migration of the top section of the dunes.

The above described changes of the dunes in the study area demonstrate a large spatial variation in dune development within a short stretch of coast. When looking at the annual difference maps of elevation change from year to year, it can be established that there is also a large temporal variation in the development of the dune.

Some periods showed that accumulation took place along the entire stretch just landward of the dune crests or vegetation limit, whereas other periods showed accumulation restricted to the depositional lobes of blowouts.

There is a large spatial variability as to whether erosion of the dune face will lead to equivalent accumulation leeward of the dune crest. However, changes of the area leeward of the dune crest does not occur completely independently from the changes of the dune face but it is found that there is no simple relation between the development of the dune face and the area leeward of the dune crest. The results indicate that blowouts are morphological features of importance in relation to the sediment transport from the beach to the leeside of the dune crest.

- How does aeolian sediment transport and dune development affect the safety level?

When analysing the 4.5 m contour, which is the level where a minimum dune width of 40 m must be maintained, it was found that generally, the dune becomes narrower with exception of section 1, where the 4.5 m contour is slightly widened for a part of the stretch. When comparing this to the calculation of the average width of each section at 4.5 m the same overall result emerges, namely that section 1 becomes wider and section 2-5 becomes narrower. However, even though, in some sections the dune becomes narrower at the 4.5 m contour, the dune is still much wider than the required 40 m and higher than the required 4.5 m.

Based on calculations of the total volume within the seaward boxes and the total volume within the landward boxes it is established that the total annual accumulation in landward boxes almost equals the total annual erosion in the seaward boxes. There is a general indication that the amount of sediment eroded from the dune face area is compensated for by the same amount of sediment accumulated in the area leeward of the dune crest when the entire study area is included. The development of the elevation change through the study period shows that erosion in the seaward box slightly exceeds the accumulation in the landward box until the period from 2017-2019 when the accumulation in the landward box increases and exceeds the erosion in the seaward box. This result is a positive sedimentary budget in the end of the study period when the volumes of the two boxes are added up and the volume changes through the study period cumulated. However, this is an average of the entire study area and when looking into the different sections it becomes clear that there is a large alongshore variation in the volume changes of the seaward and landward boxes.

The seaward box of section 1 shows relatively little volume decrease compared to the increase in the landward box, which is approx. six times as great. In section 2 the situation is the opposite, as the volume

deficit in the seaward box is twice the volume of accumulated sediment in the landward box. In sections 3, 4 and 5 the volumes of sediment eroded in the seaward boxes and the volume accumulated in the landward boxes are of similar magnitudes. In section 3 the amount of eroded sediment in the seaward box is slightly larger than the amount of sediment accumulated in the landward box. In sections 4 and 5 the amount of sediment eroded in the seaward box is smaller than the amount accumulated in the landward box.

The dunes are overall accumulating between 2006 and 2019 when looking at the total stretch. It is tempting to suggest that the dunes, despite retreat, are accumulating sediment and act as a sink for the aeolian sediment. This is not wrong, but when reflecting on the safety level it is important to have in mind that these volume calculations are based on relatively large areas (sections) and spatial variations can occur within a section. Blowouts cause very local changes in the dune area and are responsible for most of the accumulation in the landward box. At this point, the blowout sections have contributed positively in regards of catching aeolian sediment. The 4.5 m contour is not directly affected by the blowouts as the 4.5 m contour is not found to retreat into the deflation basins, thereby further narrowing the safety level at 4.5 m. Nevertheless, these morphological features present a possible contradiction as on one hand they direct the sediment into the leeside of the dunes, but on the other hand, concentrate the sediment accumulation in specific locations.

The dunes are naturally changed by accumulation and erosion of sediments and there have been decreasing width of the 4.5 m contour for almost the entire study area, but the sedimentary budget between 2006 and 2019 shows a slight accumulation. Since it is possible to analyse along the entire stretch of dunes with the LiDAR scans, it is found that the volumes are not evenly distributed along the stretch. The stability in safety level is primarily maintained, or even improved at blowout sections, while areas in-between only rarely show volume increase and landward migration of the leeside 4.5 m contour. The outline of the dunes have changed significantly e.g. in section 3, where the blowouts have caused a significant retreat of the dune top but there is only one section which shows signs of an actual increase in retreat of the dune face 4.5 m contour as a result of deflations basins of blowouts.

The dynamics of blowouts, their behaviour and how they are initially formed have not been analysed in detail in this study but they have proved to be efficient sediment accumulators. This could be further analysed and possibly utilized in future planning and dune management of areas with space for the dunes to develop naturally across shore.

- How does the sedimentary budget of the dune area contribute to the overall profile development and the general coastal sedimentary budget?

In this case, the spatial availability of data covers the entire dune field for more than a decade. This makes it possible to assess the sedimentary budget and the actual exchange of sediment between dune face area and the area leeward of the dune crest with a higher resolution than before. Despite the obvious errors in the data, calculations in this report and in Krogh (2019) are performed on planimetrical measurements rather the in transects for every 100 m. The spatial resolution allows for more detailed alongshore analyses where linear assumptions between profile measurements are no longer necessary, which may increase the accuracy.

Previous analyses of the coastal development have assumed that sediment accumulated landward of the dune top have been considered negligible. This study shows that considerable amounts of sediment accumulate leeward of the dune crest. Sections landward of the dune crest, in some areas, act as sediment sinks. The addition of sediment in the area leeward of the dune crest should be accounted for in analyses of the coastal development, at least when available data offers the possibility of assessing the volume. Including the sediment accumulation landward of dune crest would affect a calculated sedimentary budget.

It can be difficult to extract the effect of the sedimentary budget on the profile development, since this

study finds large spatial variations in the dune development. However, the overall tendency is that the dune face has been exposed to erosion and the area leeward of the dune crest has been exposed to accumulation. Deflation basins of blowouts are present along the foredune, with depositional lobes of accumulating sediment landward of it. The analysis of the 4.5 m contour indicated slight parallel displacement along some of the dune field. Other stretches indicated actual retreat and narrowing of the dune, but fluctuations in the width was evident along the full stretch, represented by both increase and decrease over time. Despite overall retreat in the 4.5 m contour, the volume above the 4.5 m contour increased for three of five sections. A large spatial variation in morphological changes was found with different combinations of retreating/advancing dune face, dune height increase, inland migration of leeside 4.5 m contours, landward migration of dune top and seaward migration of the dune face.

8. Conclusion

Accumulation of sand in the dune area is primarily found on the lee side of the dune crest and in the depositional lobe of blowouts. Erosion is primarily found at the dune face and in the deflation basin of blowouts.

- Which areas of the dune are dominated by erosion and accumulation, respectively?

The seaward boxes generally show a decrease in volume. The dune face occasionally advance and increase in volume but generally the dune face is retreating and erosion is the dominating process in this area. Main erosion within the dune range takes place in the deflation basins of blowouts. An exception is erosion in inland blowouts, developing in the middle of the dune range independently of the dune face.

The landward boxes show a general increase in sediment volume. Sediment accumulates leeward of the dune crest. The largest accumulations of sediment are located in depositional lobes of blowouts leeward of the deflation basins. However, deflation basins migrate into the landward boxes over time.

Sheets of deposited sediment are present along the entire dune crest. Periods 10 and 11 (2017-2019) show remarkable increase in sediment for most of the stretch but the factors responsible for this are unknown until further analysing.

The wind climate affects the amount of sediment eroded and accumulated in the dune area. The shape and orientation of the accumulated sediment reflect the dominating wind direction.

- What effects does the wind climate have on development of the dunes?

There is a large variation in the orientation of the blowouts, although there are no north facing blowouts. Depositional lobes have similar orientation to their respective deflation basins.

There is no direct correlation found between wind speed and accumulation or erosion of sediment. Aeolian sediment transport and dune development are complex processes and there are multiple possible restraining and attributing factors, which have not been included in this study.

Aeolian transport of sediment and the presence of blowouts can cause considerable changes in the dune area, which in turn affects the safety level.

- Do volume and dune morphology change during the study period and is development on the lee side equivalent to that of the dune face?

During the study period from 2006 to 2019 large volumes of sediment have been transported in the dune area leading to significant morphological changes of the study area.

The development of the area leeward of the dune crest is to some extend dependent on the development of the dune face area, especially if we consider blowouts, which connect the area seaward and landward of the dune crest by creation of deflation basins and depositional lobes. Though dune face retreat is encountered on much of the stretch, the retreat is not equal to a corresponding decrease in dune width, as inland migration of the leeside contours are taking place in some areas. In areas where inland migration is not taking place the retreating dune face naturally reduces the dune width and affects the safety level. It is found that there is a large spatial and temporal variation in the dune width, and development of the lee side is not necessarily equivalent to the development of the dune face, which would have caused a parallel displacement of the dune.

- How does aeolian sediment transport and dune development affect the safety level?

For some parts of the study area accumulation of sediment landward of the dune crest have ensured maintenance or even increase of the safety level, whereas the dune width have decreased in other areas. The geometry of the dune is found to be determined by local morphological changes such as develop-

ment in cross dune blowouts, and the effects are not necessarily evenly distributed along the study area. Despite retreating dune face in most of the study area and a decrease in dune width, in general, the volume is found to increase and the same applies to the dune height.

The impact of dune development on safety level varies and both local increase and decrease in safety level is found as a result of aeolian sediment transport and dune face erosion. However, the dune face retreat as a result of acute marine erosion is found to be far more influential than erosion of the dune caused by aeolian processes. Despite changes in the dune area it is found that the dune width and dune height still meets the required safety level of the study area.

- How does the sedimentary budget of the dune area contribute to the overall profile development and the general coastal sedimentary budget?

Generally, the dune face has been exposed to erosion leading to retreat of the dune face, while sediment has accumulated in the area leeward of the dune crest. However, the profile development is largely influenced by the presence of blowouts, and the study area has been exposed to large spatial and temporal variations.

It is found that large amounts of sediment have been transported across the dune crest during the study period and accumulated in the area leeward of the dune crest. This indicates that aeolian sediment transport across the dune top cannot be ignored when calculating the sedimentary budget of a coastal area.

The overall sedimentary budget of the study area is positive during the study period, mostly due to the large volume increase between 2017 and 2019. However, there are alongshore variations, which could be attributed to morphology, topography, etc., but the individual factors responsible for the variations cannot be elaborated on or explained from the studies carried out for this report as these parameters needs further investigation.

9. Perspectives

This study has provided knowledge on aeolian sediment transport and natural dune development, which can be used in future dune management and implementation of building with nature methods in relation to strengthening of dune safety and securing maintenance of the safety level. Moreover, it can be used for future implementation of natural measures, e.g. by allowing blowouts to develop naturally, in areas with sufficient space, in order to lead sediment to the area leeward of the dune crest for strengthening of the dune. Furthermore, knowledge on the effect of natural dune development on the safety level can contribute to future building with nature measures in the coastal area.

9.1 Further studies

This study has confirmed that aeolian processes and dune development are complex processes, which are affected by many factors, and only a few of them have been included in this study. It would be interesting for future studies to look into some of the factors that may have a significant impact on aeolian processes and dune development, such as the sediment source, beach area, the effect of topographic steering, dune height or stoss slope. Furthermore, it would be interesting to include measurements of the local wind regime in order to obtain a more detailed description of the forces creating aeolian sediment transport and dune development.

In further studies it would be useful to look more closely into the sediment source and limiting factors including lag deposits, as these factors affect the amount of aeolian transported sediment, thus leading to an actual aeolian transport that is smaller than the potential transport estimated from the wind velocities. Together with more detailed wind measurements this would increase the understanding of the interdepending parameters and possibly improve the correlation between the wind velocities above threshold for aeolian sediment transport and the amount of eroded and accumulated sediment.

The analyses carried out in the scope of this study have shown that there is a large spatial and temporal variability in the beach area. Therefore, it would be relevant to include the beach area in future studies in order to further investigate the effect of the beach width and state on aeolian sediment transport and dune development.

This study further indicates that topographic steering might have a significant impact on the wind and near surface flow, a factor that would be relevant to look further into in relation to development of dunes and blowouts.

The LiDAR data set have provided a significant amount of data in much higher resolution and better coverage than before. Despite disadvantages in the data setup, there is much more knowledge to be gained from these data. A slope and aspect analysis in relation to wind patterns and erosion/accumulation over time would be interesting, as this would potentially increase the understanding of the significance of topography.

Moreover, there were some indications that the stoss slope and dune height may have an impact on the amount of sediment transported from the beach to the area leeward of the dune crest. This have not been included in this study but it could be interesting to analyse this in more depth in order to find out if a provoked change in dune slope or dune height could ease the transport over the dune crest. This could possibly be used as a building with nature method in areas where the dune would benefit from an increase in volume with a view to strengthening of the dune and increasing the safety level.

Being able to utilize the presence of blowouts as a morphological feature creating accumulations of sediment could lead to volume increase in specific areas where strengthening of the dunes is sought. The development of blowout sections could seem fairly simple, but as we have seen in this report, the

complexity of initiation, position, attributing factors, and many more parameters are poorly understood. Therefore, in order to control these enormous natural phenomena and ensure the appropriate development by modification of the pathway further analysis is necessary.

Bibliography

Bagnold, R. A., 1954. The Physics of Blown Sand and Desert Dunes. s.l.:Methuen and Co. .

Bauer, B. et al., 2009. Aeolian sediment transport on a beach: Surface moisture, wind fetch, and mean transport. Geomorphology, pp. 106-116.

Bauer, B. O. & Davidson-Arnott, R. G., 2002. A general framework for modeling sediment supply to coastal dunes including wind angle, beach geometry, and fetch effects. Geomorphology, pp. 89-108.

Bauer, B. O. et al., 2012. Wind direction and complex sediment transport response across a beach-dune system. Earth Surface Processes and Landforms, pp. 1661-1677.

Christiansen, M. B. & Davidson-Arnott, R., 2004. Rates of Landward Sand Transport over the Foredune at Skallingen, Denmark and the Role of Dune Ramps. Danish Journal of Geography, pp. 31-43.

Davidson-Arnott, R., 2010. Introduction to Coastal Processes and Geomorphology. s.l.:Cambridge University Press.

Davidson-Arnott, R. G. D. et al., 2008. The effects of surface moisture on aeolian sediment transport threshold and mass flux on a beach. Earth Surface Processes and Landforms, pp. 55-74.

de Vries, S., Arens, S. M., de Schipper, M. A. & Ranasinghe, R., 2014. Aeolian sediment transport on a beach with a varying sediment supply. Aeolian Research, pp. 235-244.

ESRI, 2019. www.desktop.arcgis.com. [Online] Available at: https://desktop.arcgis.com/en/arcmap/10.3/tools/spatial-analyst-toolbox/h-how-zonal-statistics-works.htm

Hesp, P., 2011. Dune Coasts. In: Treatise on Estuarine and Coastal Science. s.l.:Waltham: Academic Press, pp. 193-221, vol 3.

Jungerius, P. D., Witter, J. V. & van Boxel, J. H., 1991. The effects of changing wind regimes on the development of blowouts in the coastal dunes of the Netherlands. Landscape Ecology, pp. 41-48, vol. 6, no. 1/2.

Krogh, M. B., 2019. Morphological evolution of a dune area at Sdr. Holmsland Tange, Denmark, s.l.: University of Copenhagen, Faculty of Science.

Kystdirektoratet, 2018. Building with Nature: Systems Description of Skodbjerge, s.l.: Danish Coastal Authority.

Masselink, G., Hughes, M. G. & Knight, J., 2011. Introduction to Coastal proceses & coastal geomorphology. 2nd ed. New York: Hodder Education.

New Jersey Sea Grant Consortium, 2016. Dune Manual, s.l.: s.n.

Ries, O., 2019. Numerical simulations of acute dune erosion under storm conditions with MIKE 21 IG, Skodbjerge, Denmark, s.l.: Danish Coastal Authority.

Walker, I. J., Hesp, P. A., Davidson-Arnott, R. G. D. & Ollerhead, J., 2006. Topographic Steering of Alongshore Airflow over a Vegetated Foredune: Greenwich Dunes, Prince Edward Island, Canada. Journal of Coastal Research, pp. 1278-1291, vol. 22, no. 5, .

Appendix A – Yearly orthophotos

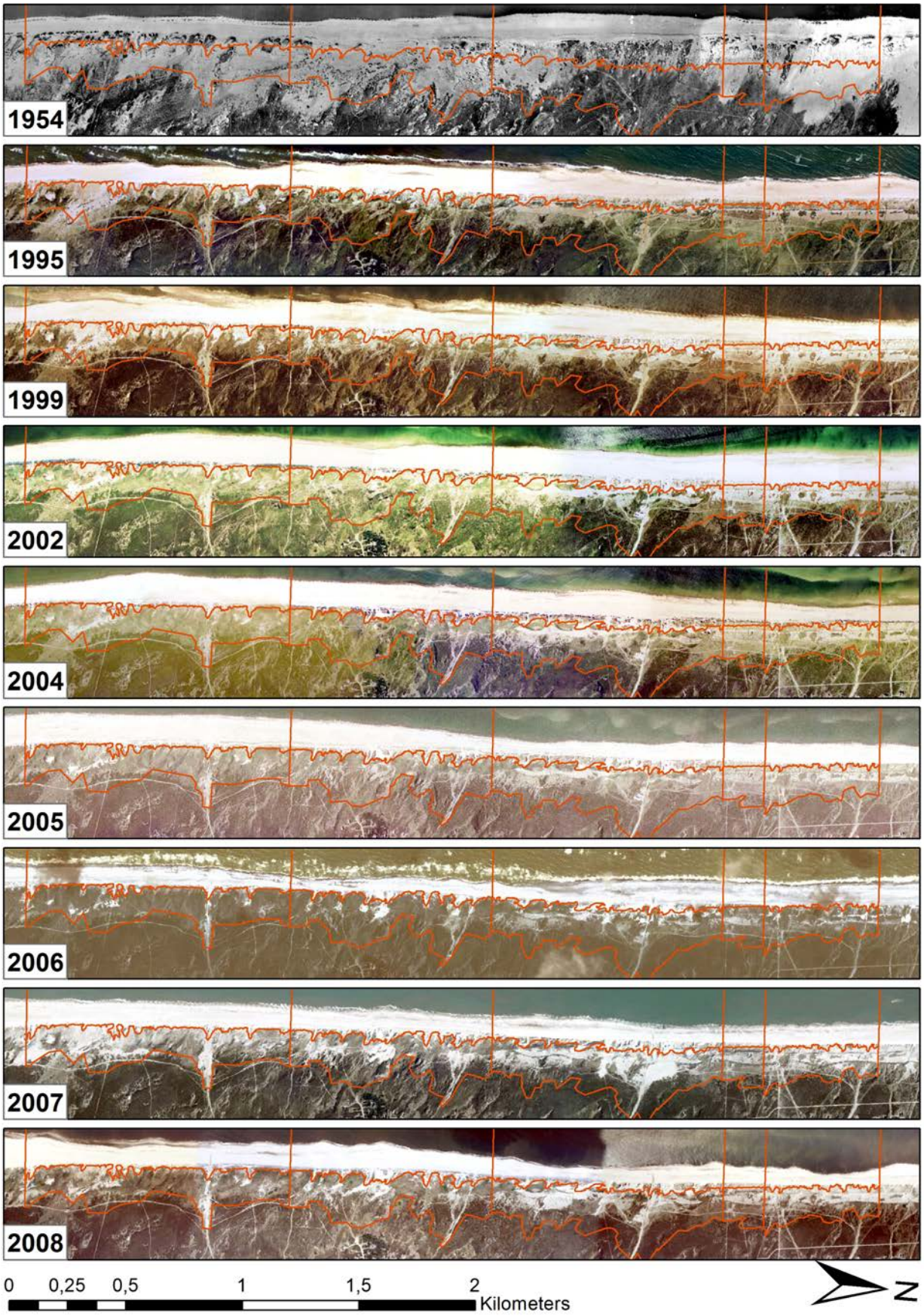

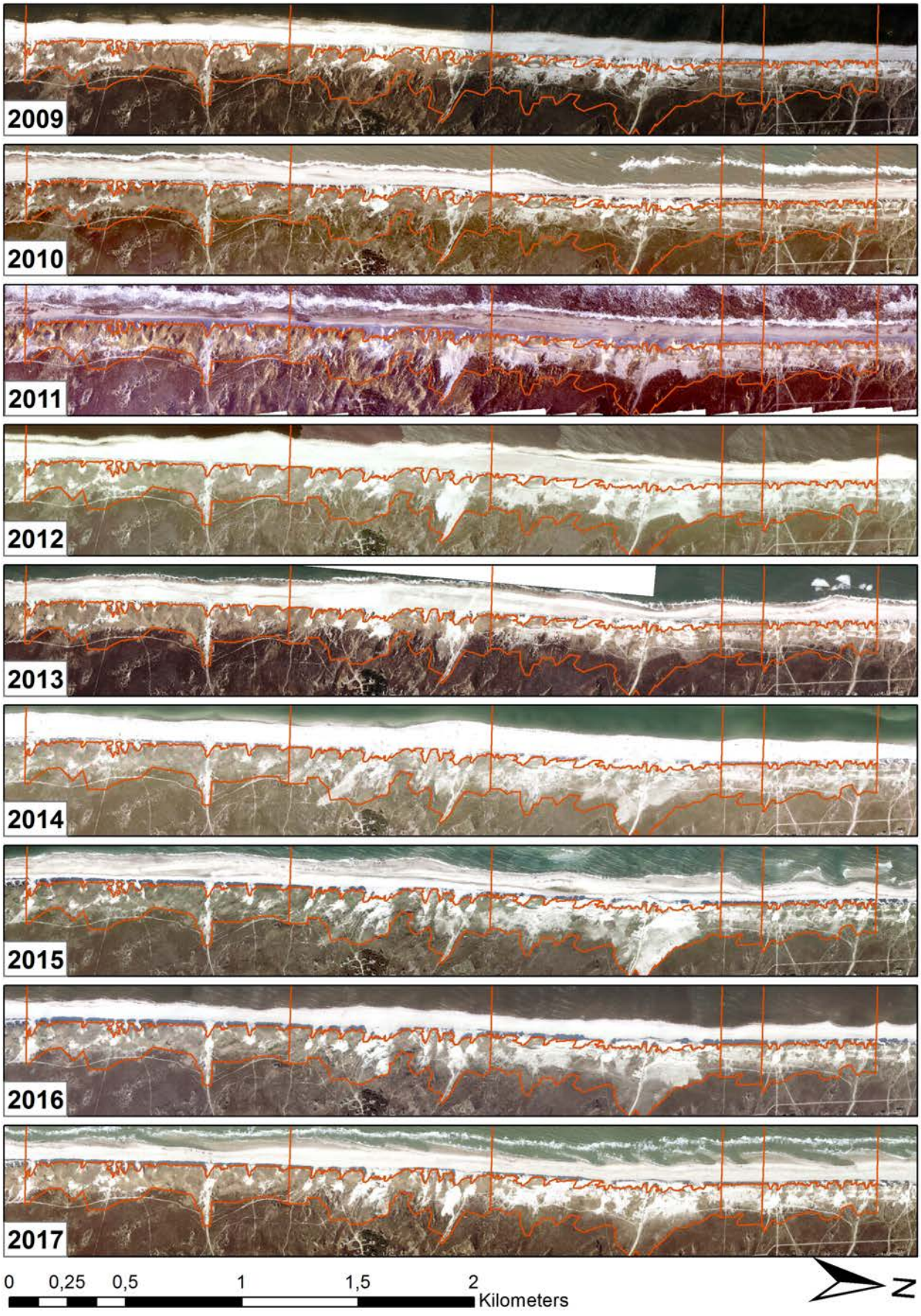
2009
2010
2011
2012
2013
2014
2015
2016
2017
0
0,25
0,5
1
1,5
2
Kilometers
N

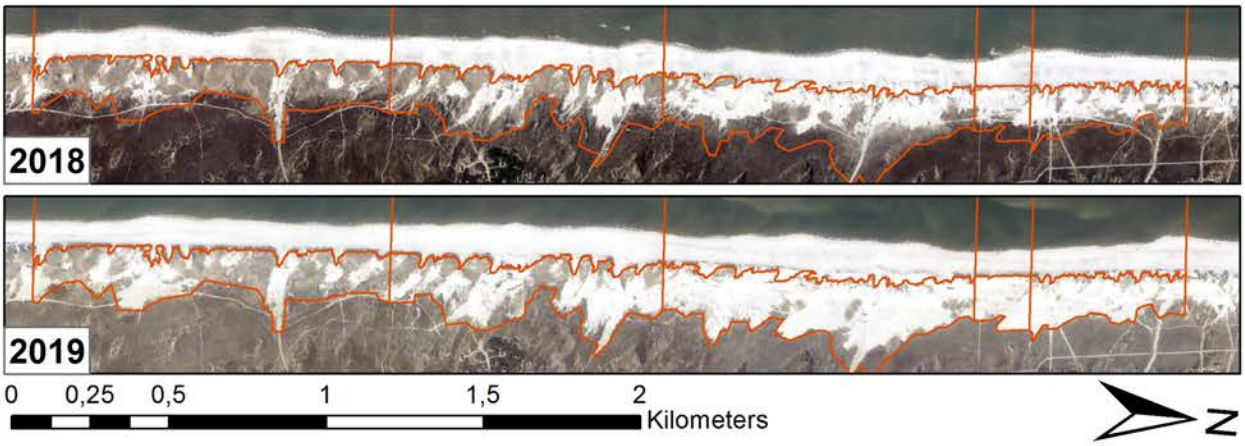
2018
2019
0
0,25
0,5
1
1,5
2
Kilometers
N

Appendix B – Volume change in each section relative to 2006

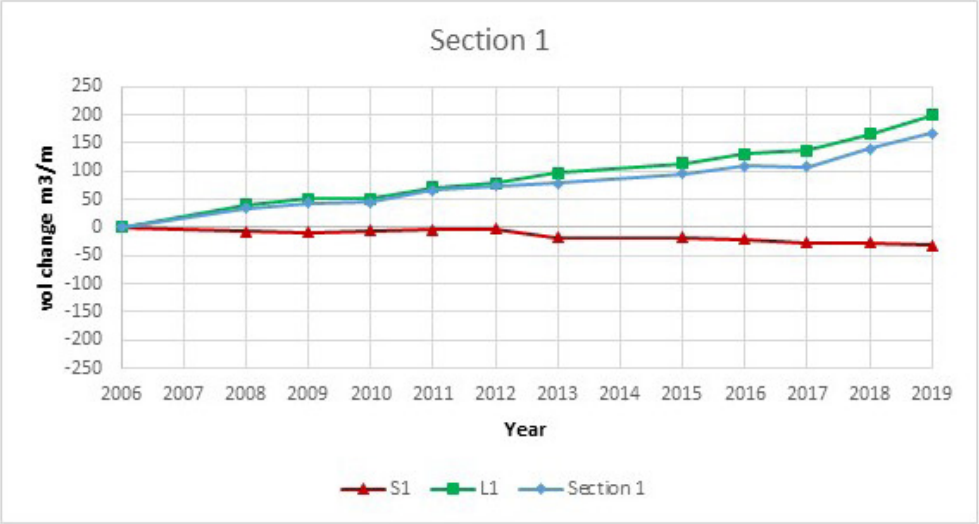

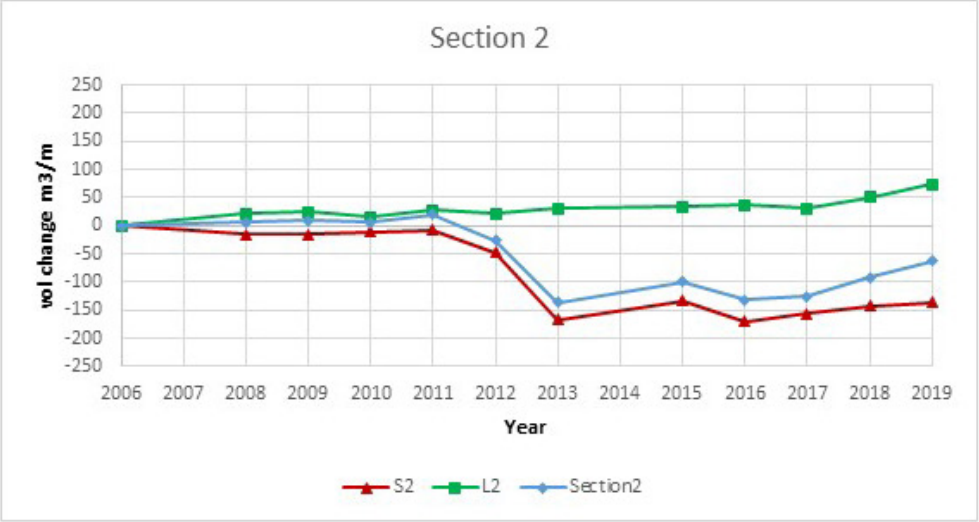

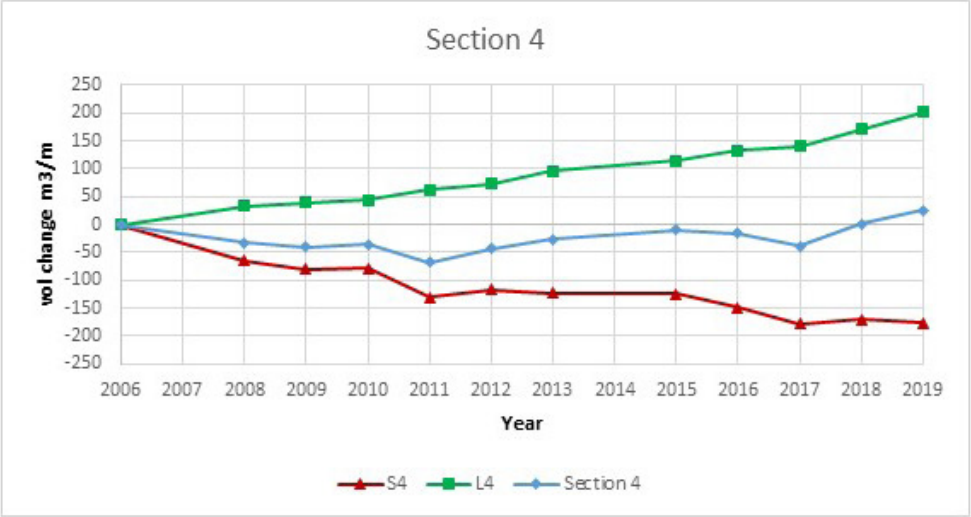
Section 4
vol change m3/m
250
200
150
100
50
0
-50
-100
-150
-200
-250
2006 2007 2008 2009 2010 2011 2012 2013 2014 2015 2016 2017 2018 2019
Year
S4
L4
Section 4

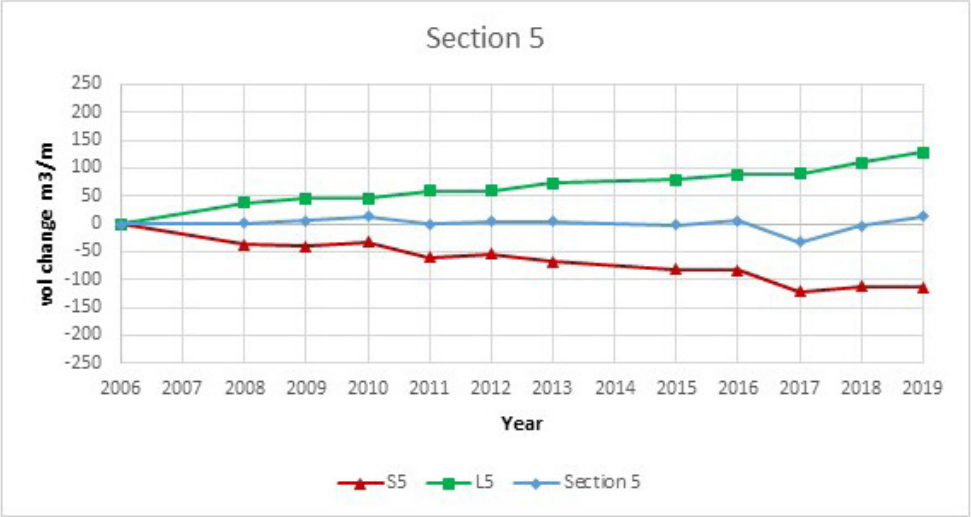
Section 5
vol change m3/m
250
200
150
100
50
0
-50
-100
-150
-200
-250
2006 2007 2008 2009 2010 2011 2012 2013 2014 2015 2016 2017 2018 2019
Year
S5
L5
Section 5

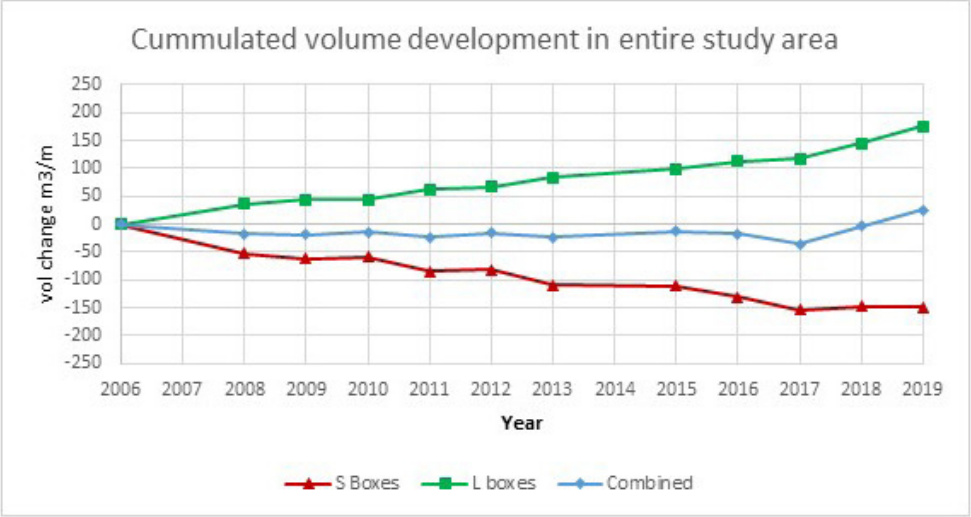
Cummulated volume development in entire study area
vol change m3/m
250
200
150
100
50
0
-50
-100
-150
-200
-250
2006 2007 2008 2009 2010 2011 2012 2013 2014 2015 2016 2017 2018 2019
Year
S Boxes
L boxes
Combined

Appendix C – Correlation test of wind and sediment transport

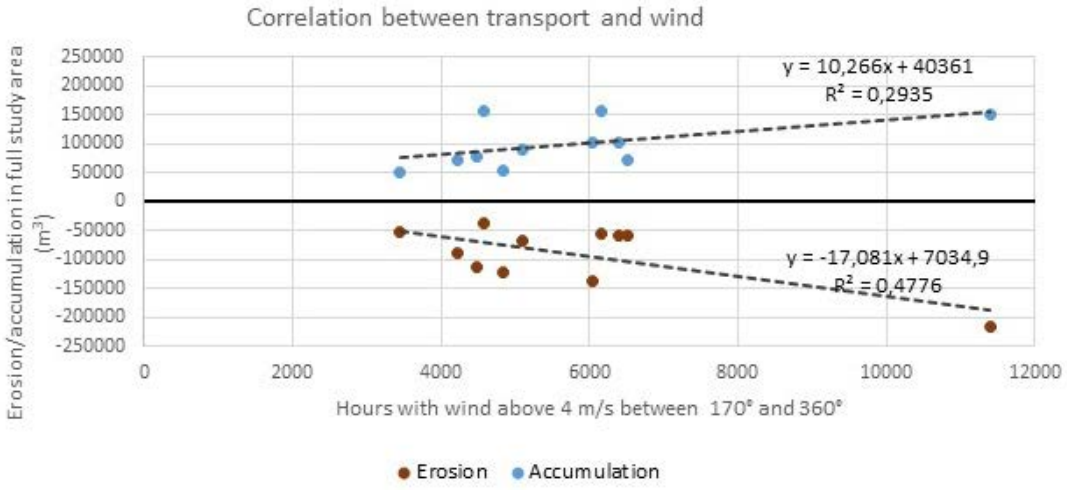

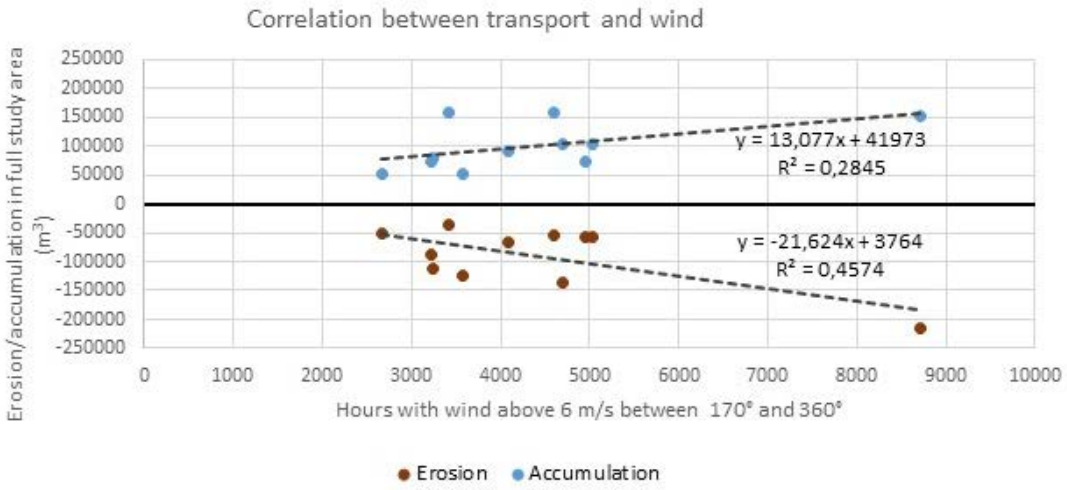

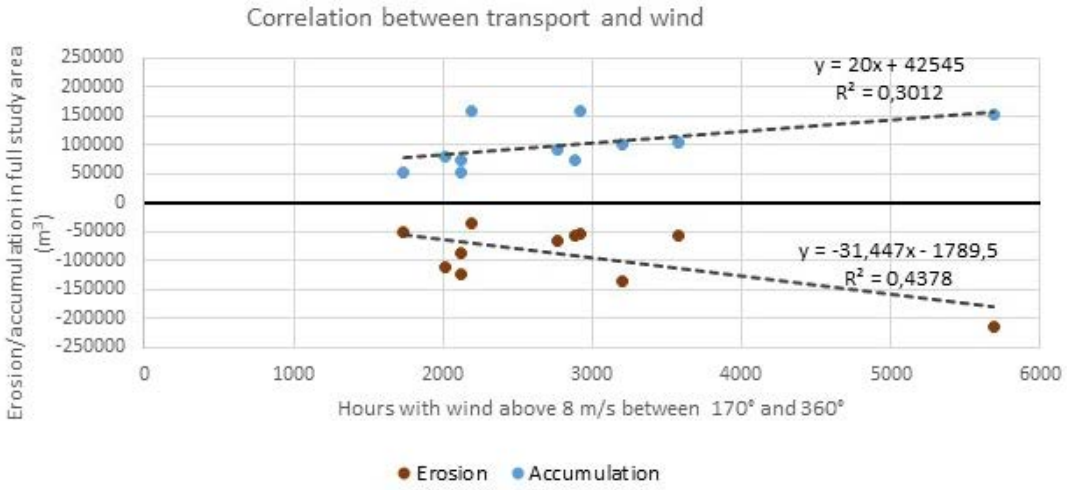

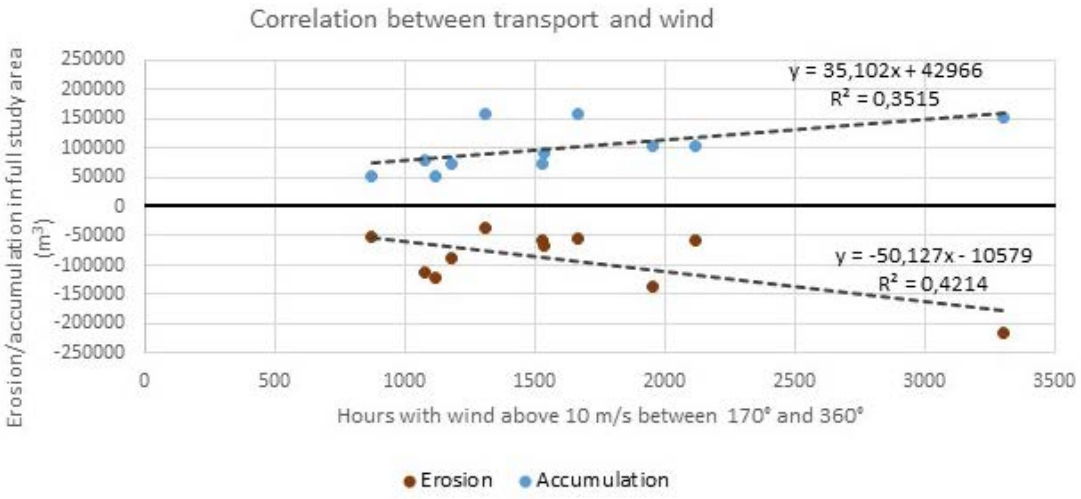
Correlation between transport and wind
y = 35,102x + 42966
R² = 0,3515
y = -50,127x - 10579
R² = 0,4214
Erosion/accumulation in full study area (m³)
Hours with wind above 10 m/s between 170° and 360°
Erosion
Accumulation

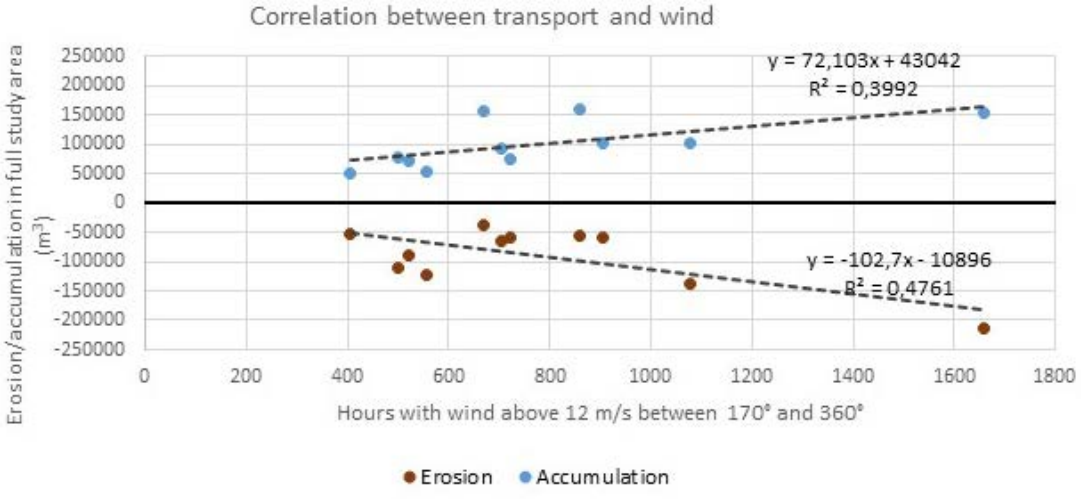
Correlation between transport and wind
y = 72,103x + 43042
R² = 0,3992
y = -102,7x - 10896
R² = 0,4761
Erosion/accumulation in full study area (m³)
Hours with wind above 12 m/s between 170° and 360°
Erosion
Accumulation

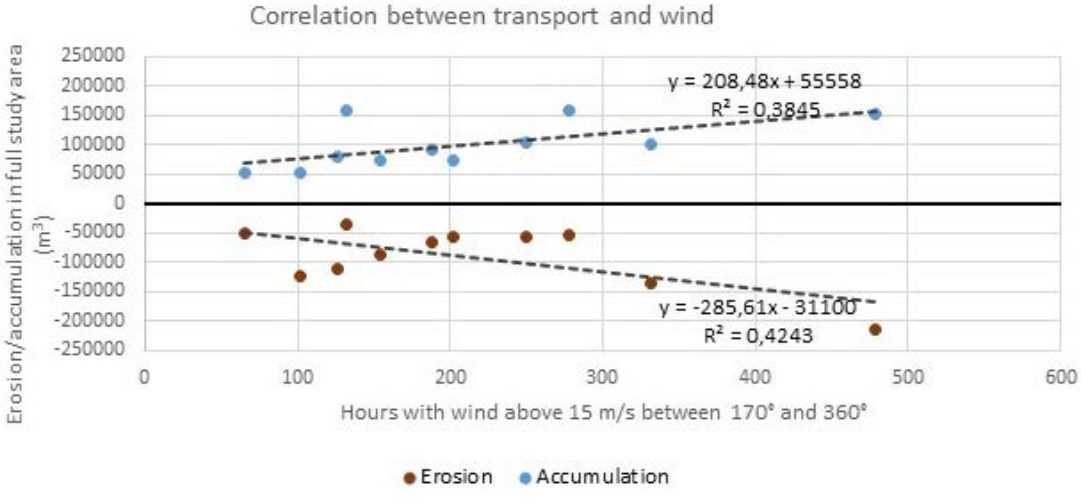
Correlation between transport and wind
y = 208,48x + 55558
R² = 0,3845
y = -285,61x - 31100
R² = 0,4243
Erosion/accumulation in full study area (m³)
Hours with wind above 15 m/s between 170° and 360°
Erosion
Accumulation

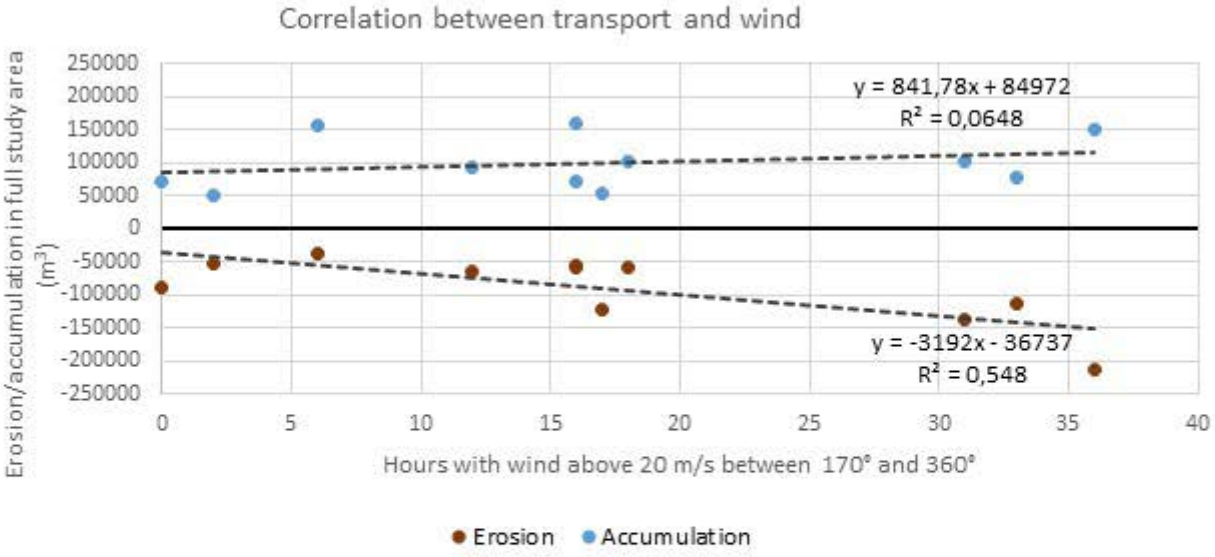
Correlation between transport and wind
Erosion/accumulation in full study area (m³)
250000
200000
150000
100000
50000
0
-50000
-100000
-150000
-200000
-250000
0
5
10
15
20
25
30
35
40
y = 841,78x + 84972
R² = 0,0648
y = -3192x - 36737
R² = 0,548
Hours with wind above 20 m/s between 170° and 360°
Erosion
Accumulation

Kystdirektoratet
Højbovej 1
7620 Lemvig
www.kyst.dk